Committee of Fukushima Medical University, the Ethical Committee of Kobe City Medical Center General Hospital, the Ethical Committee of Ozaki Eye Hospital, the Ethical Committee of the Otsu Red Cross Hospital, the Ethical Committee of Nagahama City Hospital, and the Ethical Committee at Aichi Cancer Center). All of the patients were fully informed about the purpose and procedures of this study, and written consent was obtained from each.

In this study, 401 patients with typical AMD and 510 patients with PCV were recruited from the Department of Ophthalmology at Kyoto University Hospital, Fukushima Medical University Hospital, and Kobe City Medical Center General Hospital. The control group included 2 populations: (1) 336 individuals who underwent cataract surgery and had no age-related maculopathy (ARM) (Control 1) were recruited from the Department of Ophthalmology, Kyoto University Hospital, Ozaki Eye Hospital, Japanese Red Cross Otsu Hospital, and Nagahama City Hospital; and (2) 1194 healthy individuals who were recruited from the Aichi Cancer Center Research Institute as the general population control (Control 2). AMD and ARM were defined according to the International Classification System for ARM and AMD [22]. The diagnosis of PCV was based on indocyanine green angiography, which showed a branching vascular network that terminated in polypoidal swelling. Typical AMD were late AMD which showed classic choroidal neovascularization (CNV), occult CNV, or both. All diagnoses were made by 3 retina specialists (K.Y., A.T., and A.O.); a fourth specialist (N.Y.) was consulted when the subtype classification could not be decided on by the initial 3 reviewers. All of the subjects were unrelated and were of the Japanese descent.

Genomic DNAs were isolated from the peripheral blood of the subjects by using a DNA extraction kit (QuickGene-610L, Fujifilm, Minato, Tokyo, Japan). The samples of all the patients with typical AMD and PCV and of cataract patients were genotyped using a Taqman single nucleotide polymorphism (SNP) assay with the ABI PRISM 7700 system (Applied Biosystems, Foster City, CA). The individuals recruited from the Aichi Cancer Center Research Institute were genotyped using Illumina Human-Hap 610 chips (Illumina Inc., San Diego, CA).

Linkage disequilibrium (LD) structures across the *SERPING1* gene were compared between the Caucasian and Japanese populations, using genotype data retrieved from the HapMap CEU and JPT data sets [23]. The retrieved data were loaded into Haploview to estimate LD parameters and to identify haplotype blocks [24]. Deviations in genotype distributions from the Hardy–Weinberg equilibrium (HWE) were assessed using the HWE exact test. Statistical analyses for differences in the observed genotypic distribution were performed by the chi square test for trend; logistic regression analysis was performed for age and gender adjustments. The statistical power calculation was performed using QUANTO version 1.2 [25]. P values less than 0.05 were considered statistically significant.

Results

The demographic details of the study population are presented in Table 1. Because all SNPs of the *SERPING1* gene are in the same haplotype block, rs2511989 was selected as the haplotype-tagging SNP; rs2511989 was reported to be associated with the risk of AMD in previous studies [16,19] (Fig. 1). Details of allele and genotype counts and summary statistics for rs2511989 are shown in Table 2. The success rate of genotyping of rs2511989 was 98.1%, and the distributions of the genotypes for all study groups were in the Hardy–Weinberg equilibrium ($P>0.05$). Although we compared the genotype distributions of rs2511989 in typical AMD and PCV patients against 2 independent control groups (cataract patients without ARM and healthy Japanese individuals), *SERPING1* rs2511989 was not significantly associated with typical AMD ($P = 0.932$ and 0.513, respectively); furthermore, it was not significantly associated with PCV ($P = 0.505$ and 0.141, respectively). After correction for age and gender differences based on a logistic regression model, the difference in the genotype distributions remained insignificant ($P>0.05$). Table 3 shows the odds ratios adjusted for age and gender under various genetic models. We could not find a significant association in any genetic model.

Next, we calculated our statistical power to detect an association of a risk allele with the odds ratio reported in the previous study that investigated the association of rs2511989 with developing AMD. When we targeted the original study reported by Ennis (odds ratio 0.63) [16], our sample size had more than 90% power to detect the association (Table 2). In addition, the statistical power calculation revealed that our sample size could detect the gene-disease association for an odds ratio of 0.797 by more than 80%.

Discussion

In the present study, we investigated whether *SERPING1* gene variants are associated with typical AMD or with PCV in a Japanese population. We selected rs2511989 as the haplotype-tagging SNP, because this has been reported to be positively associated with the risk of AMD in Caucasians. The results of this study showed that *SERPING1* rs2511989 was not associated with the risk for typical AMD in a Japanese population; thus, the results did not support the hypothesis that an association between the *SERPING1* gene and AMD exists. Our sample size had more than 90% power to detect the association determined in the previous

Table 2. *SERPING1* rs2511989 Genotypic Distributions and Results of Association Tests and Power Analysis.

						vs Control 1			vs Control 2		
		GG	GA	AA	MAF	P Value	Adjusted P*	Power†	P Value	Adjusted P*	Power†
Cases	tAMD	293	102	6	0.142	0.932	0.687	93.6%	0.513	0.860	99.3%
	PCV	380	125	5	0.132	0.505	0.855	95.7%	0.141	0.678	99.2%
Controls	Control 1	248	76	10	0.144	-	-	-	-	-	-
	Control 2	859	308	27	0.152	-	-	-	-	-	-

tAMD, typical age-related macular degeneration; PCV, polypoidal choroidal vasculopathy; MAF, minor allele frequency.
*Adjusted for age and gender.
†Statistical power for detecting the association reported in the previous study (odds ratio 0.63).
doi:10.1371/journal.pone.0019108.t002

Table 3. Odds Ratios in Various Genetic Models.

Group	Model	Adjusted Odds Ratio (95% Confidence Interval)*	
		vs tAMD	vs PCV
Control 1	Additive	0.938 (0.687–1.281)	0.972 (0.72–1.312)
	Dominant	1.283 (0.746–2.204)	0.598 (0.338–1.056)
	Recessive	0.934 (0.783–1.114)	1.283 (0.746–2.204)
Control 2	Additive	1.034 (0.716–1.491)	0.933 (0.673–1.294)
	Dominant	0.940 (0.470–1.879)	0.709 (0.349–1.440)
	Recessive	1.025 (0.839–1.254)	0.983 (0.823–1.174)

*Adjusted for age and gender.
tAMD, typical age-related macular degeneration; PCV, polypoidal choroidal vasculopathy.
doi:10.1371/journal.pone.0019108.t003

study in a Caucasian cohort (odds ratio 0.63) [16]. Furthermore, we found no evidence to support the role played by *SERPING1* rs2511989 in the susceptibility to PCV, and this finding is in agreement with that of the previous study in a Chinese population [21].

The reported association between AMD and *SERPING1* rs2511989 is shown in Table 4. The size of our Japanese cohort was similar to that of the original study [16]. Furthermore, the statistical power calculation revealed that our sample size could detect the gene-disease association for an odds ratio of 0.797 by more than 80%. Had there been a true protective effect of *SERPING1* gene variants for developing AMD at the same level as was reported in previous studies [16,19], the statistical power of our study would have detected such an association. Differences in the ethnicities of subjects might be 1 reason for the difference observed between the results of this study in a Japanese cohort and those of the previous study in a Caucasian cohort. Frequency of the minor allele of rs2511989 was reportedly greater in the earlier study in a Caucasian population than that of the present study in a Japanese population. In fact, in reference to the allele frequency data from the HapMap, all genetic variants across the *SERPING1* gene showed smaller minor allele frequency in Japanese than in Caucasians.

Another possible explanation for the differences between our findings and those of other studies in different ethnic cohorts may include a difference in the phenotypes of AMD. Numerous studies have reported that distinguishing features of Asian AMD include male predominance, unilateral presentation, comparatively low incidence of soft drusen, and greater prevalence of neovascular AMD and PCV [26–29]. To address these concerns, we classified AMD patients into those with typical AMD and those with PCV, but the possible hidden differences in the phenotypes cannot be excluded. Alternatively, considering the fact that genetic variants that are associated with a particular disease in 1 population may not necessarily be associated in another population [30–32]; moreover, it is possible that gene-disease association of *SERPING1* in populations from East Asia is very weak or absent as compared with Caucasian populations.

In this study, we used general population-based controls (Control 2). The possibility exists that some of the eyes in the control 2 group might have or develop AMD or PCV, and this might be a possible explanation for the negative results in this study. However, because the prevalence of AMD in the general population is estimated to be 0.5% in the Japanese population [33], the loss of the statistical power of association analysis must be negligible. In addition, we also performed a subset analysis on

Table 4. Comparison of Association Observed between AMD and *SERPING1* rs2511989.

Subject Group		Current Study (JP)			Mayo Subjects (US)		AREDS Subjects (US)		Ennis et al. (UK)		Ennis et al. (US)		Lee et al. (US)		Lu et al. (CH)	
Subjects		Case	Control 1	Control 2	Case	Control	Case	Control	Case	Control	Case	Control	Case	Control	Case	Control
No. of participants		401	336	1194	470	310	1221	295	479	479	248	252	556	256	194	285
Allele count	G	688	572	2026	569	363	1435	357	597	500	322	282	669	283	336	493
	A	114	96	362	371	257	1007	233	355	454	174	222	413	229	52	69
Genotype count	GG	293	248	859	179	103	436	115	191	132	100	79	213	74	147	215
	GA	102	76	308	211	157	563	127	215	236	122	124	273	135	42	63
	AA	6	10	27	80	50	222	53	70	109	26	49	70	47	5	3
MAF		0.142	0.144	0.152	0.395	0.415	0.412	0.395	0.373	0.475	0.351	0.441	0.382	0.447	0.134	0.123
P values		-	0.932	0.513	-	0.46	-	0.41	-	5.4×10^{-6}	-	0.0037	-	0.011	-	0.61

MAF, minor allele frequency.
doi:10.1371/journal.pone.0019108.t004

controls 2 with 55 years of age or older to minimize the possibility that some of the eyes in the control group might develop AMD or PCV. However, no new significant differences in the genotypic distributions were found in the current study (data not shown). Thus, we concluded that the result of the analysis using control 2 is valuable as reference data which supports a lack of association between *SERPING1* and both typical AMD and PCV in a Japanese population. Another limitation is about geographical difference of Control 1, which may influence genetic background of the participants. However, because the Japanese population has been reported to have a rather small genetic diversity, according to data from the SNP discovery project in Japan [34], geographical difference should not be affect our statistical results.

In conclusion, this study showed a lack of association between *SERPING1* and both typical AMD and PCV in a Japanese population; thus, the results suggest that *SERPING1* does not play a significant role in the risk of developing AMD or PCV in Japanese.

Acknowledgments

We thank the patients and the controls who participated in this study, as well as Takahisa Kawaguchi at the Center for Genomic Medicine/Inserm U.852 for his assistance in data management. We also thank the following clinicians for their help in the recruitment of patients and controls for our study: Dr. Hiroshi Tamura and Dr. Sotaro Ooto, Kyoto University Hospital; Dr. Yasuo Kurimoto, Kobe City Medical Center General Hospital; Dr. Kuniharu Saito, Fukushima Medical University; Dr. Mineo Ozaki, Ozaki Eye Hospital; Dr. Shoji Kuriyama, Otsu Red-Cross Hospital; and Dr. Yoshiki Ueda, Nagahama City Hospital.

Author Contributions

Conceived and designed the experiments: IN KY HN NY. Performed the experiments: IN NG HN HH. Analyzed the data: IN RY. Contributed reagents/materials/analysis tools: IN KY RY NG HN HH AT AO MS TI AO KM KT FM NY. Wrote the paper: IN KY RY.

References

1. Klein R, Klein BE, Jensen SC, Meuer SM (1997) The five-year incidence and progression of age-related maculopathy: the Beaver Dam Eye Study. Ophthalmology 104: 7–21.
2. Klein RJ, Zeiss C, Chew EY, Tsai JY, Sackler RS, et al. (2005) Complement factor H polymorphism in age-related macular degeneration. Science 308: 385–389.
3. Edwards AO, Ritter R, 3rd, Abel KJ, Manning A, Panhuysen C, et al. (2005) Complement factor H polymorphism and age-related macular degeneration. Science 308: 421–424.
4. Haines JL, Hauser MA, Schmidt S, Scott WK, Olson LM, et al. (2005) Complement factor H variant increases the risk of age-related macular degeneration. Science 308: 419–421.
5. Yang Z, Camp NJ, Sun H, Tong Z, Gibbs D, et al. (2006) A variant of the HTRA1 gene increases susceptibility to age-related macular degeneration. Science 314: 992–993.
6. Dewan A, Liu M, Hartman S, Zhang SS, Liu DT, et al. (2006) HTRA1 promoter polymorphism in wet age-related macular degeneration. Science 314: 989–992.
7. Seitsonen S, Lemmela S, Holopainen J, Tommila P, Ranta P, et al. (2006) Analysis of variants in the complement factor H, the elongation of very long chain fatty acids-like 4 and the hemicentin 1 genes of age-related macular degeneration in the Finnish population. Mol Vis 12: 796–801.
8. Gotoh N, Nakanishi H, Hayashi H, Yamada R, Otani A, et al. (2009) ARMS2 (LOC387715) variants in Japanese patients with exudative age-related macular degeneration and polypoidal choroidal vasculopathy. Am J Ophthalmol 147: 1037–1041.
9. Hayashi H, Yamashiro K, Gotoh N, Nakanishi H, Nakata I, et al. (2010) CFH and ARMS2 Variations in age-related macular degeneration, polypoidal choroidal vasculopathy, and retinal angiomatous proliferation. Invest Ophthalmol Vis Sci 51: 5914–5919.
10. Simonelli F, Frisso G, Testa F, di Fiore R, Vitale DF, et al. (2006) Polymorphism p.402Y>H in the complement factor H protein is a risk factor for age related macular degeneration in an Italian population. Br J Ophthalmol 90: 1142–1145.
11. Sho K, Takahashi K, Yamada H, Wada M, Nagai Y, et al. (2003) Polypoidal choroidal vasculopathy: incidence, demographic features, and clinical characteristics. Arch Ophthalmol 121: 1392–1396.
12. Terasaki H, Miyake Y, Suzuki T, Nakamura M, Nagasaka T (2002) Polypoidal choroidal vasculopathy treated with macular translocation: clinical pathological correlation. Br J Ophthalmol 86: 321–327.
13. Kondo N, Honda S, Kuno S, Negi A (2009) Coding variant I62V in the complement factor H gene is strongly associated with polypoidal choroidal vasculopathy. Ophthalmology 116: 304–310.
14. Gotoh N, Yamada R, Nakanishi H, Saito M, Iida T, et al. (2008) Correlation between CFH Y402H and HTRA1 rs11200638 genotype to typical exudative age-related macular degeneration and polypoidal choroidal vasculopathy phenotype in the Japanese population. Clin Experiment Ophthalmol 36: 437–442.
15. Lee KY, Vithana EN, Mathur R, Yong VH, Yeo IY, et al. (2008) Association analysis of CFH, C2, BF, and HTRA1 gene polymorphisms in Chinese patients with polypoidal choroidal vasculopathy. Invest Ophthalmol Vis Sci 49: 2613–2619.
16. Ennis S, Jomary C, Mullins R, Cree A, Chen X, et al. (2008) Association between the SERPING1 gene and age-related macular degeneration: a two-stage case-control study. Lancet 372: 1828–1834.
17. Allikmets R, Dean M, Hageman GS, Baird PN, Klaver CC, et al. (2009) The SERPING1 gene and age-related macular degeneration. Lancet 374: 875–876.
18. Park KH, Ryu E, Tosakulwong N, Wu Y, Edwards AO (2009) Common variation in the SERPING1 gene is not associated with age-related macular degeneration in two independent groups of subjects. Mol Vis 15: 200–207.
19. Lee AY, Kulkarni M, Fang AM, Edelstein S, Osborn MP, et al. (2010) The effect of genetic variants in SERPING1 on the risk of neovascular age-related macular degeneration. Br J Ophthalmol 94: 915–917.
20. Lu F, Zhao P, Fan Y, Tang S, Hu J, et al. (2010) An association study of SERPING1 gene and age-related macular degeneration in a Han Chinese population. Mol Vis 16: 1–6.
21. Li M, Wen F, Zuo C, Zhang X, Chen H, et al. (2010) SERPING1 polymorphisms in polypoidal choroidal vasculopathy. Mol Vis 16: 231–239.
22. Bird AC, Bressler NM, Bressler SB, Chisholm IH, Coscas G, et al. (1995) An international classification and grading system for age-related maculopathy and age-related macular degeneration. The International ARM Epidemiological Study Group. Surv Ophthalmol 39: 367–374.
23. International HapMap Consortium (2003) The International HapMap Project. Nature 426: 789–796.
24. Barrett JC, Fry B, Maller J, Daly MJ (2005) Haploview: analysis and visualization of LD and haplotype maps. Bioinformatics 21: 263–265.
25. Gauderman WJ (2002) Sample size requirements for matched case-control studies of gene-environment interaction. Statistics in Medicine 21: 35–50.
26. Chang TS, Hay D, Courtright P (1999) Age-related macular degeneration in Chinese-Canadians. Can J Ophthalmol 34: 266–271.
27. Bird AC (2003) The Bowman lecture. Towards an understanding of age-related macular disease. Eye (Lond) 17: 457–466.
28. Mori K, Horie-Inoue K, Gehlbach PL, Takita H, Kabasawa S, et al. (2010) Phenotype and genotype characteristics of age-related macular degeneration in a Japanese population. Ophthalmology 117: 928–938.
29. Maruko I, Iida T, Saito M, Nagayama D, Saito K (2007) Clinical characteristics of exudative age-related macular degeneration in Japanese patients. Am J Ophthalmol 144: 15–22.
30. Helgason A, Pálsson S, Thorleifsson G, Grant SF, Emilsson V, et al. (2007) Refining the impact of TCF7L2 gene variants on type 2 diabetes and adaptive evolution. Nat Genet 39: 218–225.
31. Chandak GR, Janipalli CS, Bhaskar S, Kulkarni SR, Mohankrishna P, et al. (2007) Common variants in the TCF7L2 gene are strongly associated with type 2 diabetes mellitus in the Indian population. Diabetologia 50: 63–67.
32. Horikoshi M, Hara K, Ito C, Nagai R, Froguel P, et al. (2007) A genetic variation of the transcription factor 7-like 2 gene is associated with risk of type 2 diabetes in the Japanese population. Diabetologia 50: 747–751.
33. Kawasaki R, Wang JJ, Ji GJ, Taylor B, Oizumi T, et al. (2008) Prevalence and risk factors for age-related macular degeneration in an adult Japanese population: the Funagata study. Ophthalmology 115: –1381, 1381 e1371-1372.
34. Haga H, Yamada R, Ohnishi Y, Nakamura Y, Tanaka T (2002) Gene-based SNP discovery as part of the Japanese Millennium Genome Project: identification of 190,562 genetic variations in the human genome. Single-nucleotide polymorphism. J Hum Genet 47: 605–610.

ARTHRITIS & RHEUMATISM
Vol. 63, No. 10, October 2011, pp 2930–2938
DOI 10.1002/art.30485

Presumptive Role of 129 Strain–Derived *Sle16* Locus in Rheumatoid Arthritis in a New Mouse Model With Fcγ Receptor Type IIb–Deficient C57BL/6 Genetic Background

Aya Sato-Hayashizaki,[1] Mareki Ohtsuji,[2] Qingshun Lin,[1] Rong Hou,[1] Naomi Ohtsuji,[1] Keiko Nishikawa,[1] Hiromichi Tsurui,[1] Katsuko Sudo,[3] Masao Ono,[4] Shozo Izui,[5] Toshikazu Shirai,[1] Toshiyuki Takai,[4] Hiroyuki Nishimura,[2] and Sachiko Hirose[1]

Objective. **Fcγ receptor type IIb (FcγRIIb) is a major negative regulator of B cells, and the lack of FcγRIIb expression has been reported to induce systemic lupus erythematosus (SLE) in mice of the C57BL/6 (B6) genetic background. The 129 strain–derived *Sle16* locus on the telomeric region of chromosome 1 including polymorphic *Fcgr2b* confers the predisposition to systemic autoimmunity when present on the B6 background. We undertook this study to examine the effect of the *Sle16* locus on autoimmune disease in FcγRIIb-deficient B6 mice.**

Methods. **We established 2 lines of FcγRIIb-deficient B6 congenic mouse strains (KO1 and KO2) by selective backcrossing of the originally constructed FcγRIIb-deficient mice on a hybrid (129 × B6) background into a B6 background. Although both lack FcγRIIb expression, the KO1 and KO2 strains carry different lengths of the 129 strain–derived telomeric chromosome 1 segment flanked to the null-mutated *Fcgr2b* gene; the KO1 strain carries a 129 strain–derived ~6.3-Mb interval distal from the null-mutated *Fcgr2b* gene within the *Sle16* locus, while this interval in the KO2 strain is of B6 origin.**

Results. **Unexpectedly, both strains failed to develop SLE; instead, the KO1 strain, but not the KO2 strain, spontaneously developed severe rheumatoid arthritis (RA) with an incidence reaching >90% at age 12 months.**

Conclusion. **The current study shows evidence that the epistatic interaction between the *Fcgr2b*-null mutation and a polymorphic gene(s) in the 129 strain–derived interval located in the distal *Sle16* locus contributes to RA susceptibility in a new mouse model with the B6 genetic background, although the participation of other genetic polymorphisms cannot be totally excluded.**

The importance of genetic factors in rheumatoid arthritis (RA) is well characterized by the aggregation of the disease in families and the high risk of the disease, both in siblings and in genetically identical twins of affected subjects, compared with that in the general population. In addition to previous studies focusing on the contribution of the HLA–DR locus to RA, recent genome-wide screening has shown linkage of many non–major histocompatibility complex (non-MHC) regions to the disease (1,2). Despite decades of research, however, the genes controlling RA susceptibility have not been precisely identified.

In mouse models, a strong influence of the MHC region was seen in collagen-induced arthritis (CIA) (3), as observed in patients with RA. Polymorphic non-MHC genes, such as *C5, Fcgr2b, Ncf1, and Il1b*, were also suggested to affect susceptibility and severity in CIA and in the K/BxN serum–transfer model of arthritis in mice

Supported in part by a grant-in-aid for the Foundation of Strategic Research Projects in Private Universities (S0991013) from the Ministry of Education, Science, Technology, Sports, and Culture of Japan, a grant for Research on Intractable Diseases from the Ministry of Health, Labor, and Welfare of Japan, and a grant from the Swiss National Foundation for Scientific Research.

[1]Aya Sato-Hayashizaki, BS, Qingshun Lin, MD, Rong Hou, MD, Naomi Ohtsuji, BS, Keiko Nishikawa, BS, Hiromichi Tsurui, PhD, Toshikazu Shirai, MD, PhD, Sachiko Hirose, MD, PhD: Juntendo University, Tokyo, Japan; [2]Mareki Ohtsuji, BS, Hiroyuki Nishimura, PhD: Toin University of Yokohama, Yokohama, Japan; [3]Katsuko Sudo, PhD: Tokyo Medical University, Tokyo, Japan; [4]Masao Ono, MD, PhD, Toshiyuki Takai, PhD: Tohoku University, Sendai, Japan; [5]Shozo Izui, MD: University of Geneva, Geneva, Switzerland.

Address correspondence to Sachiko Hirose, MD, PhD, Department of Pathology, Juntendo University School of Medicine, 2-1-1 Hongo, Bunkyo-ku, Tokyo 113-8421, Japan. E-mail: sacchi@juntendo.ac.jp.

Submitted for publication December 9, 2010; accepted in revised form May 26, 2011.

(4–7). In murine models of spontaneously occurring RA, such as MRL/*lpr* mice, SKG mice, IL-1 receptor antagonist (IL-1Ra)–deficient mice, and gp130-mutated mice, aberrant signals to immune cells due to mutated Fas (8), ZAP-70 (9), IL-1R (10), and IL-6R gp130 (11), respectively, have been shown to contribute to pathogenesis. However, none of these RA mouse models shares such mutated genes. These findings illustrate the genetic heterogeneity of RA susceptibility, in which the effects of different sets of susceptibility genes induce the same RA phenotypes. Thus, further studies to identify additional susceptibility genes could contribute to a more thorough understanding of the genetic basis of RA.

The presence of several autoantibodies, such as rheumatoid factors (RFs) and antibodies against type II collagen (CII) and cyclic citrullinated peptide (CCP), is a characteristic feature of RA patients, and immune complexes composed of these autoantibodies have been suggested to be involved in the pathogenesis of joint inflammation. Thus, molecular mechanisms responsible for the activation of RA-specific autoantibody-producing B cells are a matter of intense investigation. Among a number of molecules controlling B cell activation, Fcγ receptor type IIb (FcγRIIb) is one of the major regulators that negatively controls B cell receptor (BCR)–mediated activation signals (12). FcγRIIb-deficient C57BL/6 (B6) mice exhibit marked serum RF activities (13), indicating the critical role of FcγRIIb in RF induction. It is also reported that the FcγRIIb deficiency renders mice highly susceptible to CIA (14,15). However, the reports by Bolland and Ravetch (16) and Nimmerjahn and Ravetch (17) indicated that FcγRIIb-deficient B6 mice did develop systemic lupus erythematosus (SLE), but not RA.

In the present study, we established 2 lines of FcγRIIb-deficient B6 congenic strains of mice. Surprisingly, one of them spontaneously developed severe RA, but not SLE, and the other failed to develop either disease. The genomic difference between the 2 strains resides in the ~6.3-Mb interval distal from the null-mutated *Fcgr2b* gene, and the interval of the RA-prone strain is of the 129 strain origin and the interval of the other is of the B6 strain origin. This 129 strain–derived interval is located within the *Sle16* locus, an ~9.3-Mb interval (18,19), which has been shown to induce susceptibility to the production of high levels of autoantibodies and the development of mild glomerulonephritis when transferred on a B6 background (18). Our studies show evidence that the 129 strain–derived interval within the *Sle16* locus confers the predisposition to RA in mice with the FcγRIIb-deficient B6 genetic background.

MATERIALS AND METHODS

Mice. Two FcγRIIb-deficient B6 congenic lines, KO1 and KO2, were obtained by backcrossing the FcγRIIb-deficient mice originally constructed on a hybrid (129 × B6) background (20) into a B6 background for 12 generations using C57BL/6NCrJ mice (Charles River Japan). Genotyping of these strains in the telomeric chromosome 1 region around the knockout FcγRIIb gene was done, taking advantage of gene polymorphisms or microsatellite markers polymorphic between the 129 and B6 strains (Figure 1). All mice were housed under identical specific pathogen–free conditions, and all experiments were performed in accordance with our institutional guidelines.

Genotyping. DNA was extracted from mouse tail tissue. Genotyping of microsatellite markers was carried out as described elsewhere (21). Genotyping of the *Fcgr2b*-null mutation was performed using polymerase chain reaction (PCR) with the forward primers 5′-AAACTCGACCCCCCGTGGATC-3′ (wild-type) and 5′-CTCGTGCTTTACGGTATCGCC-3′ (*Fcgr2b*-null) and with the reverse primer 5′-TTGACTGTGGCCTTAAACGTGTAG-3′ (common). These primer pairs give rise to a 161-bp product for the wild-type allele and a 232-bp product for the *Fcgr2b*-null allele. Polymorphism of *Fcgr3* in the B6-unique insertion and deletion sites of the α-chain was determined by length difference of the PCR

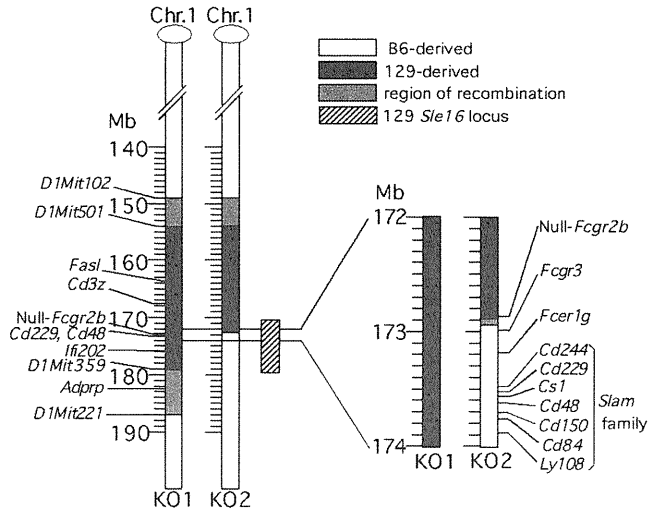

Figure 1. Genetic map of the telomeric region on chromosome 1 (Chr. 1) in two different Fcγ receptor type IIb (FcγRIIb)–deficient C57BL/6 (B6) congenic strains of mice (KO1 and KO2; see Results for description of establishment of strains). The gene segment shown by the solid bar was introduced into the B6 background from the originally constructed FcγRIIb-deficient mice on a hybrid (129 × B6) background. Genotypes were determined by analysis of microsatellite marker polymorphisms and allele polymorphisms of *Fcgr2b*, *Fcgr3*, and 2 members of the *Slam* family (*Cd229* and *Cd84*). The shaded bar represents the region of recombination between the B6 strain–derived interval (open bar) and the 129 strain–derived interval (solid bar). The hatched bar represents the reported 129 strain–derived *Sle16* locus (18,19).

products between strains 129 and B6, using the forward primer 5′-TCCATCTCTCTAGTCTGGTACC-3′ and the reverse primer 5′-AAAAGTTGCTGCTGCCACC-3′.

Polymorphisms for *Cd229* and *Cd84* were examined using single-strand conformational polymorphism. Primers for PCR were designed to amplify fragments encompassing the second exon of *Cd229* including amino acid position 130 and the second exon of *Cd84* including amino acid position 27. The forward and reverse primers used were 5′-GCAGACTCAAAGTCAGCGAAG-3′ and 5′-TGGTGAGGATAACATTCTTTTGG-3′, respectively, for *Cd229* and 5′-AAAACAATTCAACAGTGTGATGG-3′ and 5′-AAGTCCAGGCAATGTTGTCA-3′, respectively, for *Cd84*. PCR products were denatured at 98°C for 10 minutes, loaded on a 15% polyacrylamide gel, and run in 0.5× Tris–borate–EDTA using a constant-temperature control system (AB-1600 and AE-6370; Atto) at 17°C under a constant current of 20 mA/gel for 3 hours. Single-stranded DNA fragments in the gel were visualized by silver staining (Daiichi Pure Chemicals).

Scoring of arthritis. Ankle joint stiffness was examined by inspection and arbitrarily scored as follows: 0 = none, 1 = mild, 2 = moderate, and 3 = severe. Scores for both ankle joints were totaled for each mouse.

Radiography. Whole skeletal specimens were placed on shielded x-ray film and exposed to low-energy x-rays (Softex-CMB).

Histopathology and tissue immunofluorescence. For histologic examination, tissues were fixed in 4% paraformaldehyde and embedded in paraffin. Sections were stained with hematoxylin and eosin or periodic acid–Schiff and hematoxylin. Joint tissues were decalcified in 10% EDTA in 0.1*M* Tris buffer (pH 7.4). For immunofluorescence, tissues were embedded in Tissue-Tek OCT compound and frozen in liquid nitrogen. Frozen kidney sections were stained with fluorescein isothiocyanate (FITC)–labeled goat antibodies to IgG for 60 minutes at room temperature. For analysis of splenic tissues, frozen sections were 3-color stained for 30 minutes at room temperature with Alexa 488–labeled anti-CD4 and anti-CD8 monoclonal antibodies (mAb), Alexa 647–labeled anti-B220 mAb, and Alexa 546–labeled peanut agglutinin (PNA). Antibodies and PNA were purchased from BD PharMingen and Vector, respectively, and the labeling of these reagents was done in our laboratory. Color images were obtained using laser scanning microscopy (LSM 510 META; Carl Zeiss).

Serum levels of antibodies. Serum levels of RF were measured using an enzyme-linked immunosorbent assay (ELISA), as previously described (22). Briefly, an ELISA plate precoated with mouse IgG Fc fragment (OEM Concepts) was incubated with appropriately diluted mouse serum samples, washed, and then incubated with peroxidase-conjugated rat anti-mouse κ-chain antibodies (BD PharMingen). RF activities were expressed in units by reference to a standard curve obtained by serial dilution of a standard serum pool from 4–6-month-old MRL/*lpr* mice containing 1,000 unit activities/ml. Serum levels of anti-CII antibodies were measured using an ELISA plate precoated with bovine CII (Sigma-Aldrich). Serum levels of IgG anti-CCP antibodies were measured with a commercially available kit (Cosmic Corporation) using anti-mouse IgG second antibodies and were expressed as relative units according to the manufacturer's instructions. Serum levels of IgG antibodies against double-stranded DNA (dsDNA), histone, and chromatin were measured using ELISA, as previously described (23–25). Serum levels of binding activities against dsDNA, histone, and chromatin were expressed in units by reference to a standard curve obtained by serial dilution of a standard serum pool from (NZB × NZW)F_1 mice ages >8 months, containing 1,000 unit activities/ml (23–25).

Assays for cytokines. An aliquot of 1×10^6 cells/well obtained from popliteal lymph nodes was cultured for 3 days in 96-well flat-bottomed plates precoated with 10 μg/ml of anti-CD3 (145-2C11; eBioscience) and anti-CD28 (37.51; eBioscience) mAb in RPMI 1640 culture medium supplemented with 10% fetal calf serum, 45 μ*M* 2-mercaptoethanol (Invitrogen), 100 units/ml penicillin (Invitrogen), and 100 μg/ml streptomycin (Invitrogen). The levels of cytokines in the culture supernatants were measured using a standard sandwich ELISA according to the manufacturer's instructions (BD PharMingen for IL-6, interferon-γ [IFNγ], tumor necrosis factor α [TNFα], IL-4, and IL-10; eBioscience for IL-17).

Flow cytometric analysis. For the analysis of splenic lymphocytes, aliquots of 1×10^6 spleen cells were 3-color stained with phycoerythrin (PE)–labeled anti-CD4 or anti-CD8, FITC-labeled anti-B220 (6B2), and biotin-labeled anti-CD69 mAb, followed by staining with streptavidin–allophycocyanin (APC). For plasma cell analysis, spleen cells were stained with FITC-labeled anti-B220 and PE-labeled anti-CD138 mAb. For germinal center B cell analysis, cells were stained with FITC-labeled anti-B220 mAb and biotinylated PNA, followed by staining with streptavidin-APC. For follicular T helper cell phenotype analysis, spleen cells were 2-color stained with FITC-labeled anti-CD4 and PE-labeled anti–inducible costimulator (anti-ICOS) or anti–programmed death 1 (anti–PD-1) mAb. For intracellular cytokine staining, lymph node cells or cells obtained from ankle joint synovial tissues digested with 30 μl of Liberase TH (Roche Applied Science) for 1 hour at 37°C were stimulated with 0.2 μg/ml phorbol myristate acetate (PMA) and 2 μg/ml ionomycin in the presence of Golgi Plug (BD PharMingen) for 5 hours, stained with APC-labeled anti-CD4 mAb, and fixed/permeabilized using BD Cytofix/Cytoperm solution (BD PharMingen), followed by staining with PE-labeled anti–IL-17 and FITC-labeled anti-IFNγ or anti-TNFα mAb. Data were analyzed using a FACSAria flow cytometer (Becton Dickinson) and FlowJo software (Tree Star).

Measurement of urinary protein. Five microliters of urine was diluted 20 times with 0.1% Triton X-100 in distilled water and mixed with 100 μl of 2.5×10^{-5}*M* bromphenol blue solution in sodium acetate buffer, pH 3.2. The optical density at 605 nm ($OD_{605\ nm}$) of the mixture was measured, and the amounts of protein were calculated according to a standard curve obtained using bovine serum albumin solution.

Statistical analysis. Statistical analysis was carried out using the Mann-Whitney U test. *P* values less than 0.05 were considered significant.

RESULTS

Establishment of 2 lines of FcγRIIb-deficient B6 congenic mice. Two lines of FcγRIIb-deficient B6 congenic strains of mice, designated KO1 and KO2, carry

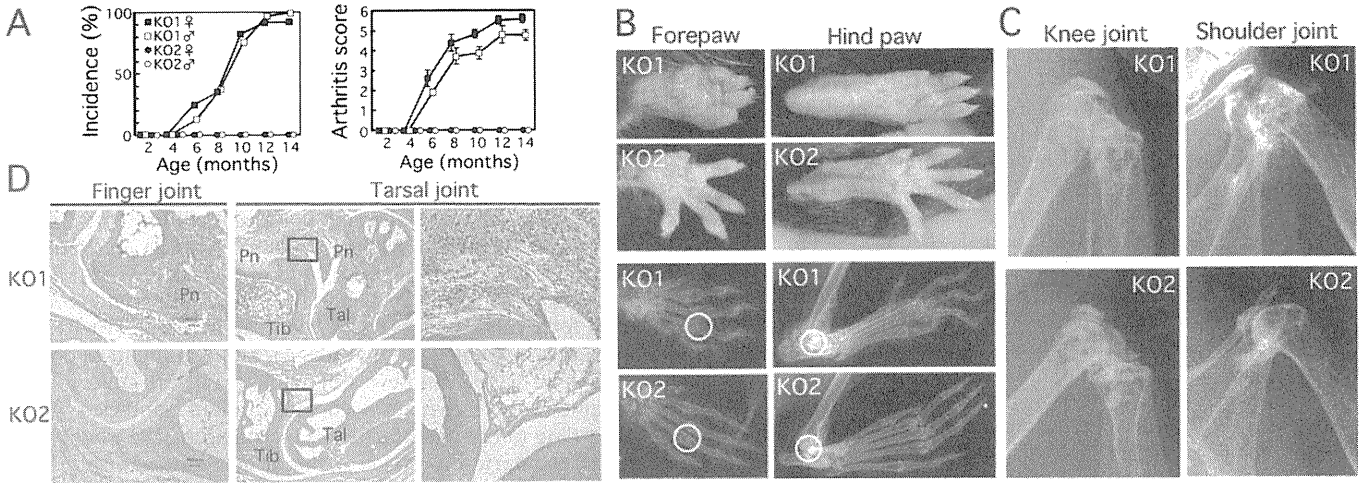

Figure 2. Comparisons of arthritis changes. **A,** Incidence of arthritis and mean ± SEM arthritis scores in KO1 mice (33 females and 30 males) and KO2 mice (15 females and 11 males). **B,** Representative macroscopic and radiographic findings in forepaws and hind paws of KO1 and KO2 mice at age 10 months. KO1 mice show marked swelling and stiffness of the wrist and ankle joints. Radiographs show the deformity of palmar and tarsal bones and finger joints. **C,** Representative radiographic findings in knee and shoulder joints of female KO1 and KO2 mice at age 10 months. The complete loss of joint space with marked destruction and resorption of bone is observed in KO1 mice. **D,** Representative histopathologic changes in finger and ankle joints of KO1 and KO2 mice (**circles** in **B**) at age 10 months. KO1 mice show marked synovitis with inflammatory cell infiltration and the destruction of bone due to pannus formation. Boxed areas in middle panels are shown at higher magnification in right panels. Results are representative of those obtained from 6 female mice in each strain. **Pn** = pannus; **Tib** = tibia; **Tal** = talus. Hematoxylin and eosin stained; original magnification × 100 in finger joint; × 40 and × 200 in tarsal joint. See Results for description of establishment of KO1 and KO2 strains.

different lengths of the 129 strain–derived telomeric chromosome 1 region flanked to the null-mutated *Fcgr2b* gene (Figure 1). The KO1 strain carries the 129 strain–derived interval from microsatellite marker *D1Mit501* to *D1Mit359*, and the KO2 strain bears the 129 strain–derived interval from *D1Mit501* to null-mutated *Fcgr2b*. In the KO2 strain, recombination occurred between the *Fcgr2b* and *Fcgr3* genes, and the region downstream of *Fcgr3* including *Slam* family genes is derived from B6 mice, thus lacking the ~6.3-Mb interval distal from the null-mutated *Fcgr2b* gene, which corresponds to the distal region of the 129 strain–derived *Sle16* locus (Figure 1). Microsatellite analysis confirmed that other autoimmune-linked 129 strain–derived intervals on chromosomes 3, 7, and 13 reported in studies using crosses between 129 and B6 strains (26) are of B6 origin in both KO1 and KO2 strains.

Spontaneous development of severe RA in KO1 mice, but not in KO2 mice. We found that KO1 mice, but not KO2 mice, spontaneously developed severe arthritis, with swelling and limited mobility of both ankle and wrist joints symmetrically after age 4 months. Severity of arthritis increased with increasing age, and the incidence was >90% at age 12 months (Figures 2A and B). There was no sex difference in the incidence of disease. Although the arthritis score tended to be higher in females than in males, the difference was not statistically significant. Radiographic examination revealed the deformity of finger joints associated with the osteoporosis and destruction/fusion of subchondral bones, particularly in the carpal and tarsal bones (Figure 2B). Large joints such as the knee and shoulder were also affected (Figure 2C), but vertebral joints were not affected. Histopathologic examination revealed severe synovitis with remarkable mononuclear cell and neutrophil infiltration and the destruction of cartilage and bone due to pannus formation in KO1 mice, but not in KO2 mice (Figure 2D). These findings clearly indicate that the distal region of the 129 strain–derived *Sle16* locus, which is absent in KO2 mice, is essential for the development of RA in KO1 mice.

Figure 3A compares serum levels of RA-associated autoantibodies, namely, RF and IgG antibodies against CII and CCP, and of SLE-associated autoantibodies, such as those against dsDNA, histone, and chromatin, among female KO1, KO2, and B6 mice at age 8 months. The levels of RA- and SLE-associated autoantibodies were significantly increased in KO1 mice compared with those in KO2 mice and in B6 mice. As for sex difference, serum RF levels in male KO1 mice were significantly lower than those seen in female KO1 mice (mean ± SEM 542 ± 43 units/ml versus 857 ± 114

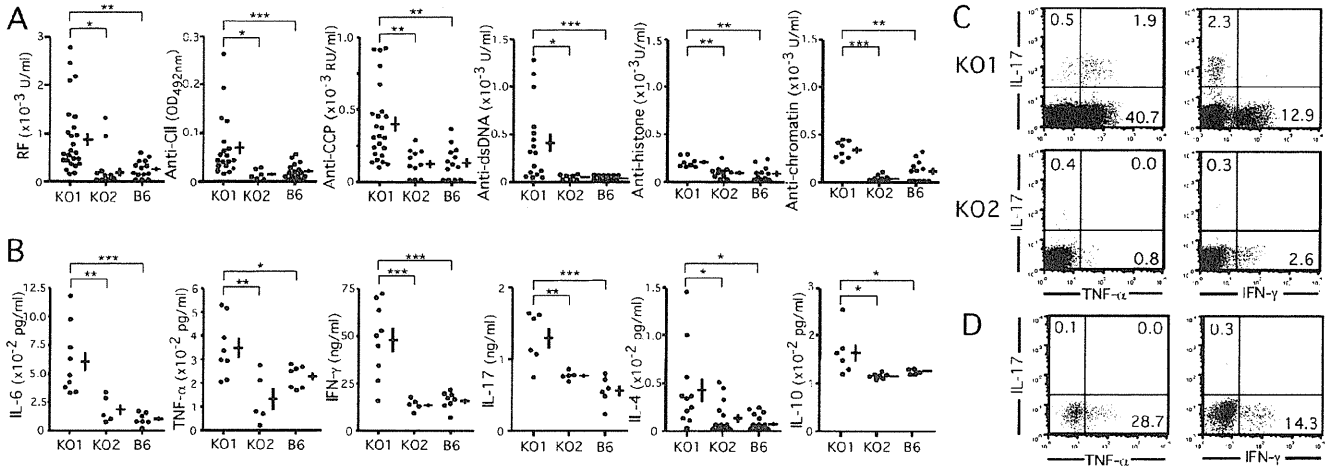

Figure 3. Comparisons of serum levels of autoantibodies and cytokine-producing potential among female KO1, KO2, and C57BL/6 (B6) mice. **A,** Serum levels of rheumatoid factor (RF) and IgG antibodies to type II collagen (CII), cyclic citrullinated peptide (CCP), double-stranded DNA (dsDNA), histone, and chromatin were compared at age 8 months. Horizontal and vertical bars represent the mean ± SEM. * = $P < 0.05$; ** = $P < 0.01$; *** = $P < 0.001$. **B,** Lymphocytes from inguinal and popliteal lymph nodes from 10-month-old mice were cultured in the presence of antibodies to CD3 and CD28 for 3 days, and the amounts of interleukin-6 (IL-6), tumor necrosis factor α (TNFα), interferon-γ (IFNγ), IL-17, IL-4, and IL-10 in the culture supernatants were measured using enzyme-linked immunosorbent assay. Horizontal and vertical bars represent the mean ± SEM. * = $P < 0.05$; ** = $P < 0.01$; *** = $P < 0.001$. **C** and **D,** Lymph node cells from arthritic KO1 mice and nonarthritic KO2 mice (**C**) or synovial tissue from the ankle joints of arthritic KO1 mice (**D**) at age 10 months were stimulated with phorbol myristate acetate/ionomycin and stained with anti-CD4 and anticytokine monoclonal antibodies, and intracellular cytokines in CD4+ T cells were analyzed. Numbers in each comparison are the percentage of total CD4+ T cells producing the cytokines (IL-17, TNFα, or IFNγ). Results are representative of those obtained from 3 independent experiments. See Results for description of establishment of KO1 and KO2 strains. OD = optical density; RU = reference units.

units/ml; $P < 0.01$); however, differences in the mean ± SEM levels of other autoantibodies between male and female KO1 mice were not statistically significant (for anti-CII, 0.04 ± 0.01 $OD_{492\,nm}$ versus 0.07 ± 0.01 $OD_{492\,nm}$; for anti-CCP, 362 ± 30 reference units [RU]/ml versus 401 ± 28 RU/ml; for anti-dsDNA, 204 ± 81 units/ml versus 409 ± 100 units/ml; for antihistone, 164 ± 29 units/ml versus 208 ± 19 units/ml; and for antichromatin, 250 ± 29 units/ml versus 336 ± 32 units/ml in males versus females).

To examine the cytokine milieu contributing to the development of arthritis, popliteal and inguinal lymph node cells from 10-month-old mice were cultured for 3 days in plates precoated with anti-CD3 and anti-CD28 mAb, and the amounts of IL-6, TNFα, IFNγ, IL-17, IL-4, and IL-10 in culture supernatants were measured using ELISA. Lymphocytes from arthritic KO1 mice exhibited a higher potential to produce all these cytokines, including the antiinflammatory cytokines IL-4 and IL-10, than those from nonarthritic KO2 and B6 mice (Figure 3B). These data were not consistent with the possibility that inflammatory responses were counteracted by an increased production of antiinflammatory cytokines in KO2 mice. We then analyzed proinflammatory cytokine–producing CD4+ T cells by staining intracellular cytokines of PMA/ionomycin-stimulated lymph node cells. As shown in Figure 3C, in arthritic KO1 mice, >40% of cells produced TNFα, and a lesser but considerable population produced IFNγ. Frequencies of IL-17–positive cells were low, and the majority of them were included in TNFα producers. In contrast, in nonarthritic KO2 mice, frequencies of cells positive for these cytokines were minimal. The analysis of the frequencies of cytokine-producing CD4+ T cells in the inflamed synovial tissues in KO1 mice showed that TNFα- and IFNγ-producing cells were again predominant (Figure 3D).

Lymphocyte activation in KO1 mice, but not in KO2 mice. KO1 mice, but not KO2 or B6 mice, displayed splenomegaly (Table 1). Flow cytometric analysis revealed that while there were no differences in the frequencies of B220+ B cells among the 3 strains of mice, the percentages of CD69+ activated B cells, PNA+ germinal center B cells, and CD138+ plasma cells were significantly higher in KO1 mice than in KO2 and B6 mice (Table 1). Examination of spleen sections under immunofluorescence revealed that the formation of germinal centers with abundant PNA+B220+ B cells

Table 1. Spleen weight and splenic lymphocyte subpopulations in KO1, KO2, and C57BL/6 (B6) mice*

	KO1	KO2	B6
Spleen weight, gm	0.26 ± 0.02†	0.12 ± 0.01	0.11 ± 0.01
Spleen cell populations, %			
B220+ B cells/total cells	48.8 ± 3.4	51.8 ± 3.4	52.2 ± 2.8
CD69+B220+ B cells/total B cells	11.7 ± 0.6‡	5.2 ± 0.7	5.1 ± 0.4
PNA+B220+ B cells/total B cells	6.9 ± 0.4‡	2.1 ± 0.6	4.0 ± 0.3
CD138+ plasma cells/total cells	2.2 ± 0.4†	0.8 ± 0.2	0.4 ± 0.1
CD4+ T cells/total cells	16.9 ± 1.3	17.6 ± 0.6	18.1 ± 0.8
CD69+CD4+ T cells/total T cells	37.4 ± 4.8§	18.1 ± 0.7	15.6 ± 0.5
CD4:CD8 T cell ratio	3.0 ± 0.7§	1.3 ± 0.03	1.4 ± 0.1

* Values are the mean ± SEM of at least 10 female mice ages 9–10 months. See Results for description of establishment of KO1 and KO2 strains. PNA = peanut agglutinin.
† $P < 0.01$ versus KO2 mice.
‡ $P < 0.005$ versus KO2 mice.
§ $P < 0.05$ versus KO2 mice.

was prominent in KO1 mice compared with KO2 and B6 mice (Figure 4A). As for T cells, while there was no difference in the frequencies of CD4+ T cells, KO1 mice showed higher frequencies of CD69+ activated T cells

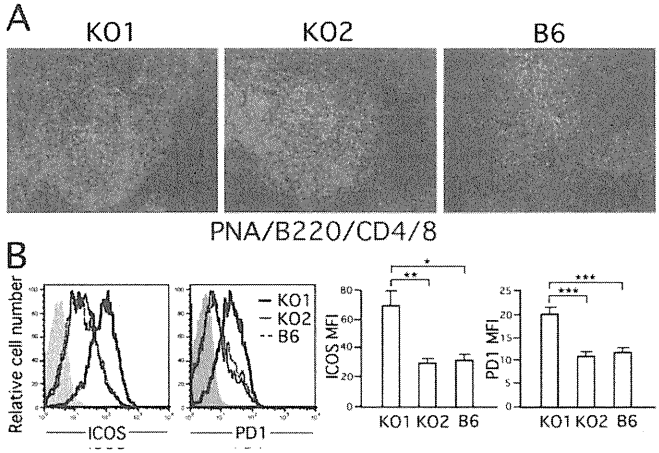

Figure 4. Spontaneous germinal center formation and increased numbers of CD4+ T cells with the follicular T helper cell phenotype in spleens of KO1 mice. **A,** Frozen sections of spleens of 10-month-old mice were triple-stained with a mixture of anti-CD4 and anti-CD8 monoclonal antibodies, anti-B220 monoclonal antibody, and peanut agglutinin (PNA) to examine the extent of germinal center formation. Results are representative of those obtained from 6 female mice in each strain. Original magnification × 200. **B,** Representative histograms of inducible costimulator (ICOS) and programmed death 1 (PD-1) expression on splenic CD4+ T cells from 10-month-old mice are shown at the left. The gray zone represents autofluorescence. The mean ± SEM mean fluorescence intensity (MFI) of ICOS and PD-1 on CD4+ T cells in KO1, KO2, and C57BL/6 (B6) mice is shown at the right. Results were obtained from 6 female mice in each group. * = $P < 0.05$; ** = $P < 0.01$; *** = $P < 0.001$. See Results for description of establishment of KO1 and KO2 strains.

with elevated CD4:CD8 T cell ratios (Table 1). In addition, CD4+ T cells in KO1 mice displayed phenotypes characteristic of follicular T helper cells, with increased expression levels of ICOS and PD-1 molecules, as compared with those in KO2 and B6 mice (Figure 4B). These findings are consistent with the report by Subramanian et al (27) demonstrating that CD4+ T cells with the follicular T helper cell phenotype were markedly expanded in autoimmune-prone B6.*Sle1.Yaa* mice, but not in nonautoimmune B6.*Yaa* mice. Because B6.*Sle1.Yaa* mice carry the autoimmune-type *Slam* family genes derived from NZW mice, the expansion of follicular T helper cells in these mice can be attributed to the autoimmune-type *Slam* family genes (27), the same types that are present in the telomeric region of chromosome 1 of KO1 mice.

No signs of lupus nephritis in either KO1 or KO2 mice. Bolland and Ravetch (16) reported that FcγRIIb-deficient B6 mice developed severe lupus nephritis with marked immune complex deposition in glomeruli. To examine the development of lupus-related glomerular lesions in our FcγRIIb-deficient B6 mice, kidney sections were stained with periodic acid–Schiff/hematoxylin or anti-IgG antibodies. As shown in Figure 5, there were no significant alterations in glomerular size and cellularity in KO1 and KO2 mice as compared to B6 mice. Minimal amounts of IgG deposits were observed only in mesangial areas of KO1 and KO2 mice at the extent comparable to those found in B6 mice. Mean ± SEM urinary protein levels remained in the normal range (<100 mg/dl) in all strains of mice, even at age 10 months, with no significant difference between strains (for KO1 mice, 76.1 ± 24.0 mg/dl; for KO2 mice, 58.2 ± 6.7 mg/dl; and for B6 mice, 42.1 ± 10.0 mg/dl).

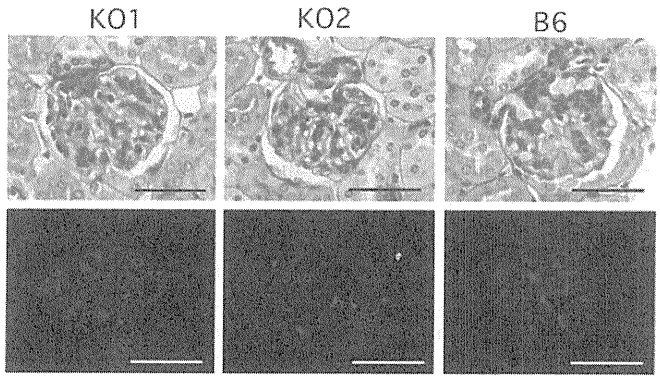

Figure 5. Histopathologic findings in glomeruli of KO1, KO2, and C57BL/6 (B6) mice at age 10 months. Top, Formalin-fixed sections were stained with periodic acid–Schiff/hematoxylin. Bottom, Frozen sections were stained with anti-mouse IgG to evaluate the deposition of IgG in renal glomeruli. Results are representative of those obtained from 6 female mice in each strain. Bars = 50 μm. See Results for description of establishment of KO1 and KO2 strains.

The development of RA is related to the 129 strain–derived interval on the telomeric region of chromosome 1 in KO1 mice. To further confirm that the development of RA is related to the 129 strain–derived interval on the telomeric region of chromosome 1 in KO1 mice, we produced (KO1 × B6)F_1 × KO1 backcross mice and examined the association of RA with the genotypes either homozygous or heterozygous for the 129 strain–derived interval on the telomeric region of chromosome 1. At age 12 months, 14 of 15 mice with the 129/129 homozygous genotype (93%) developed RA, but none of 12 mice with the 129/B6 heterozygous genotype developed RA. These results support our finding that the 129 strain–derived interval on the telomeric region of chromosome 1 in KO1 mice plays a pivotal role in RA susceptibility, although this analysis does not exclude the contribution of other genetic polymorphisms to the arthritis phenotype.

DISCUSSION

In the current study, we showed evidence that the 129 strain–derived ~6.3-Mb interval distal from the null-mutated *Fcgr2b* gene plays a pivotal role in the susceptibility to RA in FcγRIIb-deficient KO1 mice, suggesting that combined effects of the null-mutated *Fcgr2b* gene and the gene(s) in the 129 strain–derived ~6.3-Mb interval are involved in the genetic regulation of RA. Because the 129 strain–derived interval in the telomeric region of chromosome 1 contains several reported candidate genes for susceptibility to SLE (18,19), our model is useful for clarifying the genetic mechanisms that control the outcome of the separate autoimmune diseases SLE and RA.

The 129 strain–derived ~6.3-Mb interval in KO1 mice is included in the locus *Sle16* that contains several candidate genes for susceptibility to SLE, such as *Fcgr2b, Fcgr3, Slam* family genes, and IFN-inducible genes (Figure 1). There have been several reports indicating that the polymorphic *Fcgr2b* gene (21,23,28) and *Slam* family genes (19,29) are the most plausible candidate genes for susceptibility to SLE in mice.

We previously found that autoimmune-prone mice, such as NZB, MRL, BXSB, and NOD mice, share autoimmune-type *Fcgr2b* polymorphism, which has nucleotide deletion in the activating enhancer binding protein 4 binding site in the promoter region (23). Because of this type of polymorphism, the level of FcγRIIb expression on activated B cells is markedly suppressed, leading to B cell activation and enhanced pathogenic autoantibody production (21). A significant association has been reported between the polymorphism of *FCGR3A/B* and human SLE (30). However, it is still unknown whether the polymorphism of *Fcgr3* contributes to susceptibility to SLE in murine models. *Slam* family genes include *Cd244*, *Cd229*, *Cs1*, *Cd48*, *Cd160*, *Cd84*, and *Ly108* (29). The 129 strain carries autoimmune-type, haplotype 2 *Slam* family genes, the same haplotype as that reported in the autoimmune-susceptible NZB, NZW, MRL, and BXSB strains (29), which have been shown to be involved in the control of B cell tolerance (19). The IFN-inducible gene *Ifi202* was reported to be a possible candidate (31); however, recent congenic dissection studies revealed that this gene had no significant effects on susceptibility to SLE (32).

In the current study, since both KO1 and KO2 carry the null mutation of the *Fcgr2b* gene, the most plausible candidate conferring susceptibility in the locus *Sle16* is a cluster of *Slam* family genes. Although the exact susceptibility gene(s) in multiple *Slam* family genes remains undetermined, *Ly108* may be the strongest candidate. *Ly108* produces 2 splice isoforms, Ly108.1 and Ly108.2, and the autoimmune-type *Ly108* allele preferentially expresses the former in immature B cells, while the B6 type expresses the latter (29). Kumar et al (33) reported that upon BCR stimulation, immature B cells expressing Ly108.1 exhibited reduced calcium flux and decreased cell death, as compared with those expressing Ly108.2. This suggests that the Ly108.1 isoform expressed in lupus-prone mice is less effective in

the induction of clonal anergy and the deletion of immature autoreactive B cells.

Recent case–control studies in a Japanese population identified a linkage disequilibrium segment associated with RA in the chromosome 1q region containing multiple *Slam* family genes (34). Association peaks were seen at 2 functional single-nucleotide polymorphisms in *Cd244*. Investigators in that study also identified a cohort with SLE that had a genotype distribution similar to that in the RA cohorts, suggesting that CD244 plays a role in the autoimmune process shared by RA and SLE. Related to this are genome-wide linkage studies in UK and Canadian families, showing that another nearby *Slam* family gene for LY9 (*Cd229*) has risk variants for SLE (35). Further investigations in different ethnic groups are needed to clarify the roles of variants of *Slam* family genes in patients with RA and SLE.

Bolland and Ravetch (16) and Nimmerjahn and Ravetch (17) reported the development of SLE, but not RA, in their FcγRIIb-deficient B6 mouse strains. In striking contrast, not only our KO1 and KO2 mice, but also the parental mouse lines failed to develop any sign of lupus-like disease, despite the fact that our FcγRIIb-deficient B6 mice and those described by Bolland and Ravetch (16) were obtained by backcrossing the FcγRIIb-deficient mice originally constructed on a hybrid (129 × B6) background into a B6 background (20). The reason for this discrepancy remains unknown; however, identification of the reasons for this difference is extremely important in our understanding of the genetic and/or environmental mechanisms that control the outcome of the separate autoimmune diseases SLE and RA.

With regard to environmental factors, it is possible that B6 mice obtained from different commercial vendors may have different commensal intestinal bacteria, which could play an important role. Ivanov et al (36) reported that this difference affects the immune system, most strikingly, IL-17 production, which may possibly affect the severity and specificity of autoimmune disease. In addition, we cannot exclude the possibility that the development of RA, but not SLE, in KO1 mice can be influenced by additional environmental factors that are unique to our animal facility. Alternatively, a spontaneous mutation that occurred in the 129 strain–derived interval during the establishment of the KO1 strain may promote the development of RA-like joint lesions rather than lupus nephritis. Clearly, identification of the susceptibility gene(s) for RA located in the *Slam*-linked distal *Sle16* locus is of paramount importance for shedding light on the genetic mechanisms that control not only RA, but also SLE.

ACKNOWLEDGMENTS

We thank Shogo Yamamoto, Yukari Aizawa, and Kanami Fukunaga for their excellent technical assistance.

AUTHOR CONTRIBUTIONS

All authors were involved in drafting the article or revising it critically for important intellectual content, and all authors approved the final version to be published. Dr. Hirose had full access to all of the data in the study and takes responsibility for the integrity of the data and the accuracy of the data analysis.

Study conception and design. Shirai, Hirose.

Acquisition of data. M. Ohtsuji, Nishikawa, Sudo, Ono, Izui, Takai, Nishimura, Hirose.

Analysis and interpretation of data. Sato-Hayashizaki, M. Ohtsuji, Lin, Hou, N. Ohtsuji, Nishikawa, Tsurui.

REFERENCES

1. Plenge RM. Recent progress in rheumatoid arthritis genetics: one step towards improved patient care. Curr Opin Rheumatol 2009; 21:262–71.
2. Raychaudhuri S, Thomson BP, Remmers EF, Eyre S, Hinks A, Guiducci C, et al. Genetic variants at CD28, PRDM1 and CD2/CD58 are associated with rheumatoid arthritis risk. Nat Genet 2009;41:1313–20.
3. Wooley PH, Luthra HS, Stuart JM, David CS. Type II collagen-induced arthritis in mice. I. Major histocompatibility complex (I region) linkage and antibody correlates. J Exp Med 1981;154: 688–700.
4. Ji H, Gauguier D, Ohmura K, Gonzalez A, Duchatelle V, Danoy P, et al. Genetic influences on the end-stage effector phase of arthritis. J Exp Med 2001;194:321–30.
5. Johansson AC, Sundler M, Kjellen P, Johannesson M, Cook A, Lindqvist AK, et al. Genetic control of collagen-induced arthritis in a cross with NOD and C57BL/10 mice is dependent on gene regions encoding complement factor 5 and FcγRIIb and is not associated with loci controlling diabetes. Eur J Immunol 2001;31: 1847–56.
6. Hultqvist M, Olofsson P, Hormberg J, Backstrom BT, Tordsson J, Holmdahl R. Enhanced autoimmunity, arthritis, and encephalomyelitis in mice with a reduced oxidative burst due to a mutation in the Ncf1 gene. Proc Natl Acad Sci U S A 2004;101:12646–51.
7. Ohmura K, Johnsen A, Ortiz-Lopez A, Desany P, Roy M, Besse W, et al. Variation in IL-1β gene expression is a major determinant of genetic differences in arthritis aggressivity in mice. Proc Natl Acad Sci U S A 2005;102:12489–94.
8. Watanabe-Fukunaga R, Brannan CI, Copeland NG, Jenkins NA, Nagata S. Lymphoproliferation disorder in mice explained by defects in Fas antigen that mediates apoptosis. Nature 1992;356: 314–7.
9. Sakaguchi N, Takahashi T, Hata H, Nomura T, Tagami T, Yamazaki S, et al. Altered thymic T-cell selection due to a mutation of the ZAP-70 gene causes autoimmune arthritis in mice. Nature 2003;426:454–60.
10. Horai R, Saijo S, Tanioka H, Nakae S, Sudo K, Okahara A, et al. Development of chronic inflammatory arthropathy resembling rheumatoid arthritis in interleukin 1 receptor antagonist–deficient mice. J Exp Med 2000;191:313–20.
11. Sawa S, Kamimura D, Jin GH, Morikawa H, Kamon H, Nishihata

M, et al. Autoimmune arthritis associated with mutated interleukin (IL)-6 receptor gp130 is driven by STAT3/IL-7-dependent homeostatic proliferation of $CD4^+$ T cells. J Exp Med 2006;203: 1459–70.
12. Ravetch JV, Bolland S. IgG Fc receptors. Annu Rev Immunol 2001;19:275–90.
13. Moll T, Nitscehke L, Carroll M, Ravetch JV, Izui S. A critical role for FcγRIIb in the induction of rheumatoid factors. J Immunol 2004;173:4724–8.
14. Yuasa T, Kubo S, Yoshino T, Ujike A, Matsumura K, Ono M, et al. Deletion of Fcγ receptor IIB renders $H\text{-}2^b$ mice susceptible to collagen-induced arthritis. J Exp Med 1999;189:187–94.
15. Kleinau S, Martinsson P, Heyman B. Induction and suppression of collagen-induced arthritis is dependent on distinct Fcγ receptors. J Exp Med 2000;191:1611–6.
16. Bolland S, Ravetch JV. Spontaneous autoimmune disease in FcγRIIb-deficient mice results from strain-specific epistasis. Immunity 2000;13:277–85.
17. Nimmerjahn F, Ravetch JV. Antibody-mediated modulation of immune responses. Immunol Rev 2010;236:265–75.
18. Carlucci F, Cortes-Hernandez J, Fossati-Jimack L, Bygrave AE, Walport MJ, Vyse TJ, et al. Genetic dissection of spontaneous autoimmunity driven by 129-derived chromosome 1 loci when expressed on C57BL/6 mice. J Immunol 2007;178:2352–60.
19. Fossati-Jimack L, Cortes-Hernandez J, Norsworthy PJ, Cook HT, Walport MJ, Botto M. Regulation of B cell tolerance by 129-derived chromosome 1 loci on C57BL/6 mice. Arthritis Rheum 2008;58:2131–41.
20. Takai T, Ono M, Hikida M, Ohmori H, Ravetch JV. Augmented humoral and anaphylactic responses in FcγRII-deficient mice. Nature 1996;379:346–9.
21. Xiu Y, Nakamura K, Abe M, Li N, Wen XS, Jiang Y, et al. Transcriptional regulation of Fcgr2b gene by polymorphic promoter region and its contribution to humoral immune responses. J Immunol 2002;169:4340–6.
22. Abe Y, Ohtsuji M, Ohtsuji N, Lin Q, Tsurui H, Nakae S, et al. Ankylosing enthesitis associated with up-regulated IFN-γ and IL-17 production in (BXSB x NZB) F1 male mice: a new mouse model. Mod Rheumatol 2009;19:316–22.
23. Jiang Y, Hirose S, Abe M, Sanokawa-Akakura R, Ohtsuji M, Mi X, et al. Polymorphisms in IgG Fc receptor IIB regulatory regions associated with autoimmune susceptibility. Immunogenetics 2000; 51:429–35.
24. Tokushige K, Kinoshita K, Hirose S, Shirai T. Genetic association between natural autoantibody responses to histones and DNA in murine lupus. Autoimmunity 1992;12:285–93.
25. Zhang D, Fujio K, Jiang Y, Zhao J, Tada N, Sudo K, et al. Dissection of the role of MHC class II A and E genes in autoimmune susceptibility in murine lupus models with intragenic recombination. Proc Natl Acad Sci U S A 2004;101:13838–43.
26. Heidali Y, Bygrave AE, Rigby RJ, Rose KL, Walport MJ, Cook HT, et al. Identification of chromosome intervals from 129 and C57BL/6 mouse strains linked to the development of systemic lupus erythematosus. Genes Immun 2006;7:592–9.
27. Subramanian S, Tus K, Li QZ, Wang A, Tian XH, Zhou J, et al. A Tlr7 translocation accelerates systemic autoimmunity in murine lupus. Proc Natl Acad Sci U S A 2006;103:9970–5.
28. Pritchard NR, Cutler AJ, Uribe S, Chadban SJ, Morley BJ, Smith KG. Autoimmune-prone mice share a promoter haplotype associated with reduced expression and function of the Fc receptor FcγRII. Curr Biol 2000;10:227–30.
29. Wandstrat AE, Nguyen C, Limaye N, Chan AY, Subramanian S, Tian XH, et al. Association of extensive polymorphisms in the SLAM/CD20 gene cluster with murine lupus. Immunity 2004;21: 769–80.
30. Tsao BP. Lupus susceptibility genes on human chromosome 1. Int Rev Immunol 2000;19:319–34.
31. Rozzo SJ, Allard JD, Choubey D, Vyse TJ, Izui S, Peltz G, et al. Evidence for an interferon-inducible gene, Ifi202, in the susceptibility to systemic lupus. Immunity 2001;15:435–43.
32. Jorgensen TN, Alfaro J, Enriquez HL, Jiang C, Loo WM, Atencio S, et al. Development of murine lupus involves the combined genetic contribution of the SLAM and FcγR intervals within the Nba2 autoimmune susceptibility locus. J Immunol 2010;184: 775–86.
33. Kumar KR, Li L, Yan M, Bhaskarabhatla M, Mobley AB, Nguyen C, et al. Regulation of B cell tolerance by the lupus susceptibility gene Ly108. Science 2006;312:1665–9.
34. Suzuki A, Yamada R, Kochi Y, Sawada T, Okada Y, Matsuda K, et al. Functional SNPs in CD244 increase the risk of rheumatoid arthritis in a Japanese population. Nat Genet 2008;40:1224–9.
35. Cunningham Graham DS, Vyse TJ, Fortin PR, Montpetit A, Cai YC, Lim S, et al. Association of Ly9 in UK and Canadian SLE families. Genes Immun 2008;9:93–102.
36. Ivanov II, Atarashi K, Manel N, Brodie EL, Shima T, Karaoz U, et al. Induction of intestinal Th17 cells by segmented filamentous bacteria. Cell 2009;139:485–98.

European Journal of Immunology

Susceptibility loci for the defective foreign protein-induced tolerance in New Zealand Black mice: Implication of epistatic effects of *Fcgr2b* and *Slam* family genes

Takuma Fujii[1], Rong Hou[2], Aya Sato-Hayashizaki[2], Masaomi Obata[1], Mareki Ohtsuji[1], Kenichi Ikeda[1], Kenichi Mitsui[1], Yo Kodera[1], Toshikazu Shirai[2], Sachiko Hirose[2] and Hiroyuki Nishimura[1]

[1] Toin Human Science and Technology Center, Department of Biomedical Engineering, Toin University of Yokohama, Yokohama, Japan
[2] Department of Pathology, Juntendo University School of Medicine, Tokyo, Japan

In contrast to normal mice, autoimmune-prone New Zealand Black (NZB) mice are defective in susceptibility to tolerance induced by deaggregated bovine γ globulin (DBGG). To examine whether this defect is related to the loss of self-tolerance in autoimmunity, susceptibility loci for this defect were examined by genome-wide analysis using the F_2 intercross of nonautoimmune C57BL/6 (B6) and NZB mice. One NZB locus on the telomeric chromosome 1, designated Dit (*Defective immune tolerance*)-1, showed a highly significant linkage. This locus overlapped with a locus containing susceptibility genes for autoimmune disease, namely *Fcgr2b* and *Slam* family genes. To investigate the involvement of these genes in the defective tolerance to DBGG, we took advantage of two lines of *Fcgr2b*-deficient B6 congenic mice: one carries autoimmune-type, and the other carries B6-type, *Slam* family genes. Defective tolerance was observed only in *Fcgr2b*-deficient mice with autoimmune-type *Slam* family genes, indicating that epistatic effects of both genes are involved. Thus, common genetic mechanisms may underlie the defect in foreign protein antigen-induced tolerance and the loss of self-tolerance in NZB mouse-related autoimmune diseases.

Keywords: Autoimmune disease · IgG Fc Receptor · New Zealand Black mice · SLAM family · Tolerance


Supporting Information available online


See accompanying Commentary by Mitchison

Introduction

While there is diversity in immunological self-tolerant states, namely clonal deletion, anergy, or suppression of autoreactive lymphocytes, the mechanisms involved in the loss of self-tolerance may differ in different autoimmune diseases [1, 2]. Since Mitchison [3] proposed the immunological "paralysis" theory, foreign protein antigen-induced immune tolerance in vivo in mice has long been studied as a model of immunological self-tolerance (reviewed in [4]). It is well established that tolerance is inducible in adult mice by administering soluble foreign protein antigens such as bovine γ globulin (BGG) and human γ globulin (HGG) in a deaggregated form. Accumulating evidence has shown that, although both T-helper

Correspondence: Dr. Hiroyuki Nishimura
e-mail: nisimura@cc.toin.ac.jp

cells and B cells are involved in tolerance induction, the kinetics of tolerance induction differs between T and B cells, in that T-cell tolerance is achieved earlier after low-antigen doses, whereas tolerance in B cells requires more time and higher doses of tolerogens [5–7]. As the molecular mechanisms underlying these tolerance inductions have not been precisely identified, it remains elusive whether the same mechanisms are involved in the process of self-tolerance.

New Zealand Black (NZB) mice spontaneously produce autoantibodies reactive to erythrocytes and thymocytes, and autoimmune hemolytic anemia develops as these animals age (reviewed in [8]). They also produce IgM class anti-DNA antibodies and develop a mild form of immune complex-type glomerulonephritis later in life [8]. The interest in this strain as a systemic autoimmune disease model was given support by findings that, compared with findings in NZB mice, severe lupus nephritis associated with a high serum level of IgG autoantibodies develops spontaneously in the F_1 hybrid of NZB and nonautoimmune disease-prone New Zealand White (NZW) strains [9]. These findings clearly indicated that genes derived from both NZB and NZW mice contribute to this event. We previously found that the NZB locus, *Hig-1* (hyper IgG) in the telomeric region of chromosome 1, plays a pivotal role in the increased production of pathogenic IgG anti-DNA antibodies in (NZB × NZW)F_1 hybrid mice [10, 11]. *Hig-1* is tightly linked with *Fcgr2b*-encoding IgG Fc receptor IIB (FcγRIIB), a negative regulator of BCR-mediated activation signal in B cells [12, 13]. We found that *Fcgr2b* is polymorphic, and NZB *Fcgr2b* of autoimmune in nature. As the NZB-type *Fcgr2b* polymorphism has nucleotide deletions in the AP4-binding site in the promoter region, the FcγRIIB expression level on activated B cells is markedly suppressed, leading to B-cell activation and enhanced pathogenic autoantibody production [14].

In the vicinity of *Fcgr2b*, there exist polymorphic *Slam* family genes. Intensive congenic dissection studies showed that autoimmune-type *Slam* family genes play a significant role in the breakdown of self-tolerance and autoantibody production on a C57BL/6 mice (B6) genetic background [15]. As NZB mice have autoimmune-type *Slam* family genes, these genes are also suggested to contribute to the loss of self-reactive B-cell tolerance observed in autoimmune disease-prone NZB and (NZB x NZW)F_1 mice.

It has been a long time since NZB mice were found to be defective in their capacity to induce high-dose tolerance to deaggregated BGG (DBGG) [16, 17]. The defective tolerance in NZB mice was found to be an age-dependent phenomenon and preceded the onset of an autoimmune phenotypes in these mice [18]. Nevertheless, the cause–effect relationship between the defective tolerance to DBGG and the autoimmune disease of NZB mice remains unknown. In the present study, we mapped the loci responsible for the resistance to high-dose tolerance to DBGG in NZB mice in order to explore the relationship between the genetic predisposition for this defective high-dose tolerance and the autoantibody-mediated autoimmune disease.

Results

Defective immune tolerance induced by DBGG in NZB mice

We first examined whether DBGG-induced immune tolerance in our system is antigen specific. Three-month-old B6 mice were pretreated with PBS or DBGG, and immunized 1 wk later with BGG or OVA in the presence of CFA. After 1 wk, serum levels of antibodies against BGG and OVA were analyzed. Pretreatment with DBGG markedly downregulated the antibody response to BGG, but not to OVA (Fig. 1), indicating that DBGG-induced tolerance was antigen specific.

Figure 2 shows a comparison of serum levels of anti-BGG antibodies in normal B6, autoimmune-prone NZB, and (B6 × NZB)F_1 hybrid mice pretreated with DBGG or PBS and then immunized with BGG as in Fig. 1. Consistent with the earlier findings by others [16–18], NZB mice were defective in tolerance induction to DBGG, in contrast to the results in B6 mice. Tolerance induction in F_1 hybrid mice was intact as in the case of B6 mice. We then pretreated F_2 intercross mice ($n = 220$) with DBGG, immunized with BGG, and analyzed the levels of anti-BGG antibodies. Levels in F_2 intercross mice demonstrated a wide distribution, and 59% of the F_2 intercross mice showed impaired tolerance, when assuming that mice with anti-BGG antibody levels of less than 10^4 units were normal in terms of tolerance induction. These results suggest that the loci contributing to the defective tolerance are inherited in a recessive manner.

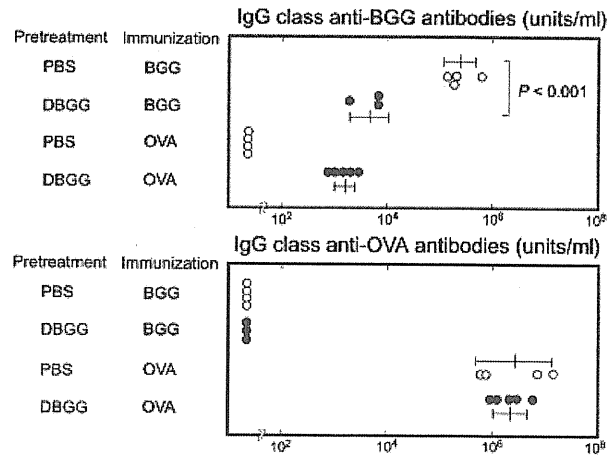

Figure 1. Antigen-specific immune tolerance induced by DBGG. Three-month-old female B6 mice were injected intraperitoneally with 10 mg of DBGG solution at days 0 and 7. Control groups of mice were injected with PBS. At day 14, mice were challenged either with BGG (250 μg) or with OVA (250 μg) emulsified in CFA in each of two hind footpads. Serum levels of IgG class anti-BGG and anti-OVA antibodies at day 21 were measured by ELISA. Pretreatment with DBGG downregulated the levels of antibodies specific to BGG but not to OVA. Closed circles and open circles show the levels of antibodies in mice pretreated with DBGG and with PBS respectively. Bars in each column represent means ± SD. The data are representative of three independent experiments.

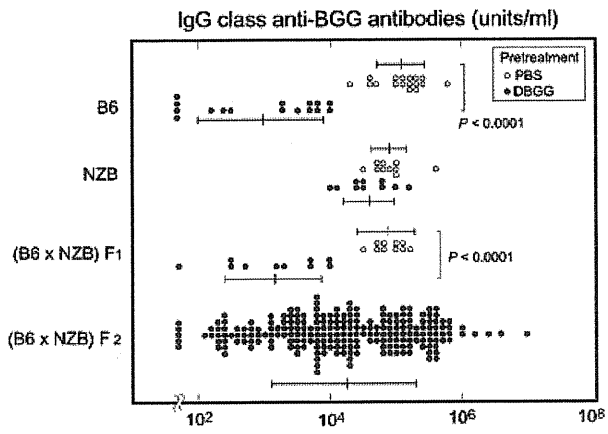

Figure 2. Serum levels of anti-BGG antibodies in B6, NZB, (B6 × NZB)F_1, and (B6 × NZB)F_2 intercross ($n = 220$) mice at day 21. These mice were pretreated with DBGG (closed circles) or with PBS (open circles), and were subsequently challenged with BGG plus CFA as in Fig. 1. Bars in each column represent means ± SD. Statistically significant differences between two groups pretreated with DBGG and PBS are shown with *p*-values in Mann–Whitney *U*-test.

Genome-wide mapping of loci for defective immune tolerance

(B6 × NZB)F_2 intercross mice were genotyped for 130 polymorphic microsatellite markers distributed on all chromosomes except the sex chromosome (markers used are shown in Supporting Information), and quantitative trait loci (QTL) regulating the levels of anti-BGG antibodies shown in Fig. 2 were mapped. Linkage analysis identified two loci on NZB chromosomes 1 and 3 (Fig. 3). The peak LOD (logarithm of odds) score for the former was 7.20 at *D1Mit15*, and the peak LOD score for the latter was 4.38 at *D3Mit109*. On the basis of the criteria for genome-wide linkage studies [19], the locus on the telomeric region of chromosome 1 showed a highly significant linkage, and that on chromosome 3 showed a significant linkage. While the former showed a single peak, a broad interval on chromosome 3 showed significant linkage, suggesting that two or more genes in this interval may be involved. The susceptibility loci linked to *D1Mit15* and *D3Mit109* are provisionally designated as *Dit* (*Defective immune tolerance*)*-1* and *Dit-2* respectively, in which *Dit-2* represents a group of genes on chromosome 3. To examine the relationship between *Dit-1* and *Dit-2*, F_2 mice with B6/B6 or NZB/NZB homozygous genotype for each of *D1Mit15* and *D3Mit109* were selected and divided into four groups according to the combination of genotypes of *D1Mit15* and *D3Mit109*, and serum levels of anti-BGG antibodies were compared (Fig. 4). The results indicated that *Dit-1* and *Dit-2* showed an additive effect on the defective induction of tolerance.

Dit-1 is located in a region that overlaps with the reported autoimmune-susceptibility genes, namely, polymorphic *Fcgr2b* [11] and *Slam* family genes [15], suggesting that a common pathway plays a role in the defective immune tolerance to foreign protein and autoantibody production.

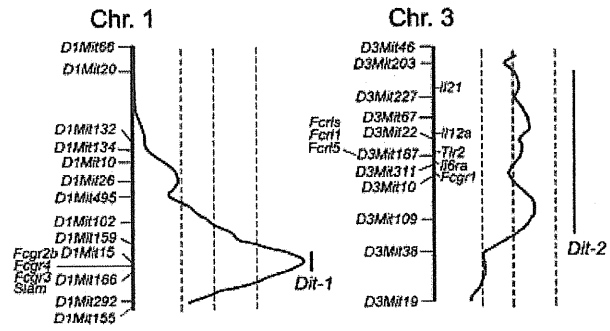

Figure 3. Loci regulating defective tolerance to DBGG obtained by genome-wide mapping in (B6 × NZB)F_2 intercross mice ($n = 220$). The three bars on each figure show the minimum criteria for "highly significant" (LOD score = 4.8), "significant" (LOD score = 3.4), and "suggestive" (LOD score = 2.0) linkages. Two loci, Dit-1 on the telomeric region of chromosome 1 and Dit-2 on chromosome 3, showed "highly significant" and "significant" linkages respectively. The black bar for Dit-1 and Dit-2 represents the one-LOD support interval.

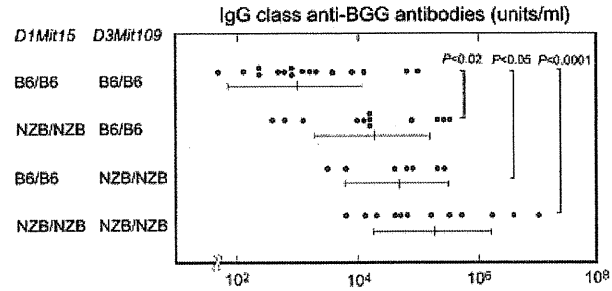

Figure 4. Comparison of serum levels of IgG anti-BGG antibodies after pretreatment with DBGG among four groups of (B6 × NZB)F_2 intercross mice. Among 220 F_2 mice, mice with B6/B6 or NZB/NZB homozygous genotype for each of D1Mit15 and D3Mit109 were selected and divided into four groups according to the combination of genotypes of D1Mit15 and D3Mit109. Bars in each column represent means ± SD. Statistically significant differences are shown with *p*-values in Scheffe's method.

Association of defective immune tolerance with autoantibody production in FcγRIIB-deficient mice

On the basis of the finding that the defective tolerance to DBGG in NZB mice is associated with the locus on chromosome 1 containing *Fcgr2b* and *Slam* family genes, we then analyzed the relationship of these genes. FcγRIIB is a negative regulator of BCR-mediated B-cell activation [12, 13] and FcγRIIB deficiency has been shown to induce autoantibody production on a B6 genetic background [20, 21]. Autoimmune-type *Slam* family genes were also reported to confer the predisposition for autoantibody production when introduced into mice with a B6 genetic background [15]. To explore the relationship between defective tolerance to DBGG and autoantibody production, we took advantage of two lines of FcγRIIB-deficient B6, established by selective backcrossing of the originally constructed FcγRIIB-deficient mice on a hybrid (129 × B6)F_1 background into B6 mice [22]. Although both strains lack FcγRIIB expression, one carries 129 strain-derived autoimmune-type *Slam* family genes

and the other carries B6-derived *Slam* family genes (Table 1). The results showed that *Fcgr2b*-deficient mice with 129 *Slam* failed to exhibit tolerance to DBGG, whereas *Fcgr2b*-deficient mice with B6 *Slam* normally exhibited tolerance to DBGG (Fig. 5A). In addition, while these two strains did not develop anti-double-stranded (ds) DNA antibody production at 3 months of age, *Fcgr2b*-deficient mice with 129 *Slam*, but not *Fcgr2b*-deficient mice with B6 *Slam*, showed significantly high serum levels of anti-dsDNA antibodies at 6 months of age (Fig. 5B). As original B6 mice are susceptible to tolerance to DBGG and do not produce anti-dsDNA antibodies, these findings clearly show that the epistatic effect of *Fcgr2b* deficiency and autoimmune-type *Slam* family genes plays a pivotal role in both the defective tolerance induction to DBGG and autoantibody production.

Discussion

Autoimmune-prone NZB mice were defective in their abilities to acquire antigen-specific tolerance when injected with tolerogenic DBGG, in keeping with the previous studies [16, 17]. In the present study, we carried out genome-wide QTL analysis using (B6 × NZB)F_2 intercross mice to map the susceptibility loci for the defective tolerance to DBGG and two NZB loci, *Dit-1* and *Dit-2* on chromosomes 1 and 3 respectively, were identified. *Dit-1* showed a peak LOD score of 7.2, which exceeded the criterion of "highly significant" linkage in genome-wide studies [19] at marker locus *D1Mit15*. *Dit-2* showed a broad interval with significant linkage, suggesting that two or more candidate genes are present in this interval.

The microsatellite marker *D1Mit15* was also reported to be a marker of the cluster of autoimmune susceptibility loci, *Hig-1/Lbw7/Nba-2/Bxs3/Sle-1*, responsible for autoantibody production and/or lupus nephritis [11, 23–26]. These findings suggest that the defective tolerance to DBGG and autoantibody production share a common process regulated by *D1Mit15*-linked

Table 1. Genotyping of the telomeric region of chromosome 1 in two lines of FcγRIIB-deficient B6 mice

Markers	Position (Mb)	FcγRIIB-deficient B6 mice with	
		129-derived *Slam*	B6-derived *Slam*
D1Mit187	115.45	B6	B6
D1Mit102	149.09	B6	129
D1Mit159	161.59	129	129
D1Mit15	170.28	129	129
Fcgr2b	172.89	Null	Null
Fcgr4	172.94	129	129
Fcgr3	172.98	129	B6
Slam family	173.48–174.40	129	B6
D1Mit359	179.21	129	B6
D1Mit221	187.04	B6	B6

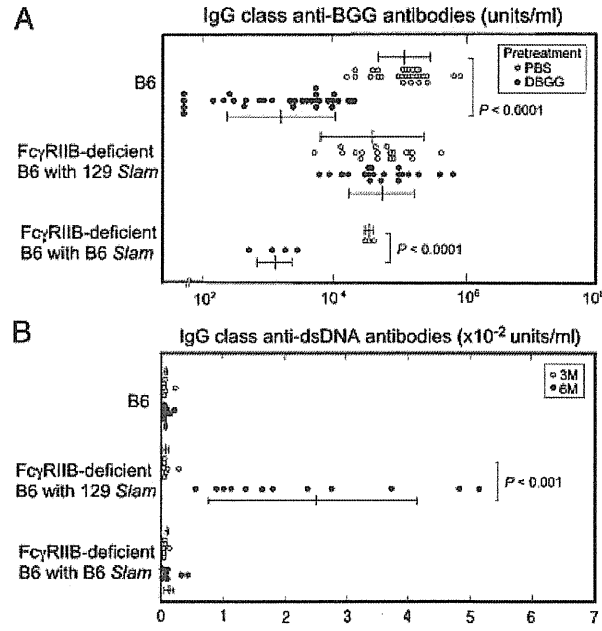

Figure 5. Defective immune tolerance and anti-dsDNA antibody production in FcγRIIB-deficient B6 mice with 129-derived *Slam* family genes. (A) B6, FcγRIIB-deficient B6 mice with 129-derived *Slam*, and FcγRIIB-deficient B6 mice with B6-derived *Slam* were tested for their abilities to exhibit tolerance by treatment with DBGG as in Fig. 1. Closed circles and open circles depict mice pretreated with DBGG and PBS respectively. (B) Comparison of serum levels of IgG anti-DNA antibodies among FcγRIIB-deficient B6 mice with 129-derived *Slam*, FcγRIIB-deficient B6 mice with B6-derived *Slam*, and B6 mice at 3 (open circles) and 6 months of age (closed circles). Bars in each column represent means±SD. Statistically significant differences are shown with *p*-values in Mann–Whitney *U*-test. The data are representative of three independent experiments.

gene(s). Among the cluster of autoimmune susceptibility loci on the telomeric region of chromosome 1, *Hig-1* [11], *Lbw7* [23], and *Nba-2* [24] were NZB loci, whereas *Bxs3* [25] and *Sle1* [26] were BXSB and NZW loci. The precise causative gene(s) linked to these autoimmune susceptibility loci has been intensively studied by establishing interval congenic strains. Accumulating evidence obtained from these studies showed that the polymorphic *Fcgr2b* [27, 28] and *Slam* family genes [15, 27] are the most likely *D1Mit15*-linked candidate autoimmune susceptibility genes. There are other plausible candidate genes in the *D1Mit15*-linked region such as *Fcgr3* and *Fcgr4* (Fig. 3). Both mouse FcγRIII and FcγRIV have similarities to the human low-affinity IgG Fc receptor, FcγRIIIA, in genomic organization and sequence characteristics [12, 13]. As *Fcgr4* is not polymorphic between the two lines of FcγRIIB-deficient B6 mice used in the present study (Table 1), this gene may not be the candidate susceptibility gene. On the contrary, *Fcgr3* is polymorphic between the two lines of mice (Table 1). In humans, the significant association has been reported between the polymorphism of *FCGR3A* and the human systemic lupus erythematosus [29]. Thus, we cannot totally exclude the possible involvement of *Fcgr3* in the loss of self-tolerance and the defective tolerance to foreign proteins; however, there have been no reports indicating that the poly-

morphism of *Fcgr3* controls the immune regulation and/or the susceptibility to autoimmune disease in murine models.

Whitmer et al. [30] showed that FcγRIIB-deficient mice are normally susceptible to the induction of tolerance by deaggregated human γ globulin (DHGG). In the present study, we found that while FcγRIIB-deficient B6 mice carrying B6-type *Slam* were susceptible to tolerance induction by DBGG, as in the case of Whitmer's report [30], FcγRIIB-deficient mice carrying 129-type *Slam* showed defective induction of tolerance to DBGG. *Slam* family genes encode several molecules, such as *Cd244*, *Cd229*, *Cs1*, *Cd48*, *Cd160*, *Cd84*, and *Ly108* [31], and the 129 strain carries autoimmune-type, haplotype 2 *Slam* family genes, the same haplotype as that reported in the autoimmune-susceptible NZB, NZW, MRL, and BXSB strains [15]. Although the exact susceptibility gene(s) in multiple *Slam* family genes remains undetermined, *Ly108* may be a plausible candidate. It has been recently shown that, in addition to two splice isoforms, Ly108-1 and Ly108-2, *Ly108* produces the third isoform, Ly108-H1, which is absent in autoimmune-type *Ly108*, and that introduction of Ly108-H1-expressing transgene markedly suppresses autoimmunity by inhibiting T-cell proliferation in mice carrying autoimmune-type *Ly108* [32]. In any instance, SLAM family molecules are expressed in a wide variety of immune cells, and the homotypic and heterotypic interactions of these cell-surface molecules induce the phosphorylation of their cytoplasmic tails, allowing the subsequent binding of signaling molecules, namely, SLAM-associated protein (SAP) and EAT2, in the cytoplasmic tail. SAP is widely expressed in T cells and EAT2 is expressed in APCs. Thus, the polymorphism of *Slam* family genes may affect the function of T cells and APCs [31]. It has been well established that the tolerance induction by deaggregated γ-globulin develops at both T- and B-cell levels [5–7]. Since SLAM signal has been shown to modulate T-cell activation mediated by signals through TCR [31], it is feasible to speculate that the polymorphism of *Slam* family genes affects the strength of the TCR-mediated signal and the subsequent T-cell response against tolerogens. Komori et al. [33] reported that SAP deficiency ameliorated autoimmune disease in the MRL/*lpr* mouse model, which is characterized by the aberrant expansion of self-reactive T cells.

On the other hand, the deficient expression of FcγRIIB in NZB mice may intrinsically contribute to the defective tolerance induction at B-cell level, since FcγRIIB is a major negative regulator of B cells and has been shown to provide a distal peripheral checkpoint to limit the accumulation of autoreactive plasma cells, thereby maintaining tolerance [34]. NZB mice have autoimmune-type *Fcgr2b* polymorphism, shared by other autoimmune-prone strains of mice, such as BXSB, MRL, and NOD [11, 35]. Because of nucleotide deletions in the AP4-binding site in the *Fcgr2b* promoter region, the FcγRIIB expression level on activated B cells in these mice is ten times lower than the level in mice carrying a nonautoimmune B6-type polymorphism [11], leading to B-cell activation and enhanced pathogenic autoantibody production [14]. Xiang et al. [36] reported that FcγRIIB controls plasma cell persistence and apoptosis and that plasma cells from autoimmune-prone mice do not express FcγRIIB and are protected from apoptosis. Consistently, it has been shown that the deletion of the *Fcgr2b* gene renders mice highly susceptible to collagen-induced arthritis (CIA) with high levels of antibodies against collagen type II [37, 38], and that *Cia9*, one of the CIA susceptibility loci, is linked to the autoimmune-type *Fcgr2* in NOD mice [39]. The importance of autoimmune-type *Fcgr2b* in the pathogenesis of autoimmunity was further supported by our earlier finding that BXSB mice congenic for B6-type *Fcgr2b* showed no evidence of autoantibody production [28].

The present study strongly suggests that the combined effect of FcγRIIB deficiency and autoimmune-type *Slam* family genes is involved in both the defective tolerance to DBGG and the loss of self-tolerance in NZB mice. The concordant relationship between defective tolerance to DHGG and autoantibody production has been reported in the studies using the BXSB strain [40]. Because of the contribution of the *Y* chromosome-linked autoimmune acceleration (*Yaa*) mutation [41], BXSB male, but not female, mice develop severe lupus nephritis associated with high serum levels of anti-DNA autoantibodies. The *Yaa* mutation is expressed functionally in B cells [42] and duplication of the *Tlr7* gene has been proposed as an etiology for *Yaa*-mediated activation of self-reactive B cells [43–45]. Chu et al. [40] reported that while male BXSB mice were resistant, female mice were susceptible to the tolerance induction by DHGG. In this respect, it is to be noted that the BXSB and NZB strains share the same autoimmune-type polymorphic *Fcgr2b* and *Slam* family genes; nonetheless, tolerance to DHGG is normally induced in female BXSB mice, in contrast to the findings in NZB mice. These findings clearly indicate that additional genes, which are present in NZB and absent in BXSB female mice, are also involved in the defective tolerance induction. While in the BXSB strain, the *Yaa* mutation exerts this effect, such genes in the NZB strain remain unidentified. The current study suggests that one possible candidate is the NZB-derived *Dit-2*-linked gene(s). The interval overlapping with *Dit-2* on chromosome 3 has been reported to be involved in the upregulation of autoantibody production; however, the causative interval is derived from normal B10 or B6 mice [25, 46], thus it may differ from the NZB *Dit-2*. There are several potential candidate genes for *Dit-2*, such as *Il21*, *Il12a*, *Tlr2*, *Il6ra*, *Fcgr1*, and a group of genes for Fcγ receptor homologues, including *Fcrl1*, *Fcrl5*, and *Fcrls* (Fig. 3). It is worth noting that the region including *Fcgr1* and a group of genes for Fcγ receptor homologues on mouse chromosome 3 is syntenic with the 1q21–q22 region, which is linked with autoimmune susceptibility loci on human chromosome 1 [29]. Among these, *Fcrl5* codes for an Fcγ receptor homologue, FcRH3, with immunoreceptor tyrosine-based inhibitory motifs in the molecule [47], and has been shown to be transcribed in marginal zone B cells [48]. However, our preliminary study did not reveal any polymorphism between the NZB and the B6 strains in the coding sequence of *Fcrl5* (data not shown); thus, further studies are needed to identify the possible candidate genes for *Dit-2*.

The present linkage analysis suggests that common genetic mechanisms are operative for both the defect in tolerance induced by foreign proteins and the loss of self-tolerance in autoantibody-mediated autoimmune diseases. Our current study supports the notion that further studies on the mechanisms underlying the defective immune tolerance to DBGG at cellular/molecular levels in autoimmune disease-prone mice may extend

our understanding of the pathogenesis of antibody-mediated autoimmune diseases.

Materials and methods

Mice

NZB and B6 mice were obtained from Sankyo Laboratory Service (Tokyo, Japan) and were maintained in the animal-care facility at Toin University of Yokohama. Male NZB and female B6 mice were mated to obtain F_1 hybrids. Female (B6 × NZB)F_2-intercross mice ($n = 220$) were used for linkage studies. Two lines of FcγRIIB-deficient B6 mice were kindly provided by Dr. Toshiyuki Takai (Institute of Development, Aging and Cancer, Tohoku University, Japan) [22] and were bred in our animal facility. These strains were maintained under specified pathogen-free conditions. The study was reviewed and approved by the research ethics committee of Toin University of Yokohama.

Antigen

BGG (Sigma Chemicals, St. Louis, MO) was dissolved in PBS (pH 7.2) at 20 mg/mL and was sterilized using a 0.45 μ filter (Schleicher & Schuell GmbH, Dassel, Germany). Tolerogenic BGG was prepared as follows [18]. The BGG solution was ultracentrifuged at 100 000 × *g* for 2 h at 4°C using a SW41Ti rotor (Beckman Instruments, Palo Alto, CA). The top half of the BGG solution was collected and subjected to a second ultracentrifugation. After the second run, the top half of the DBGG solution was immediately used as tolerogenic BGG without storage. For immunization with CFA and for ELISA, BGG was further purified using a protein G Sepharose column (Pharmacia Biotech, Piscataway, NJ). Lyophilized ovalbumin, OVA (chicken egg albumin, grade VII) was obtained from Sigma Chemicals.

Induction of tolerance

On days 0 and 7, 3-month-old NZB, B6, (B6 × NZB)F_1 and (B6 × NZB)F_2-intercross mice were injected i.p. with tolerogenic DBGG (10 mg/mouse) dissolved in PBS. Control groups of mice were injected with PBS instead of DBGG. On day 14, mice were injected with BGG (250 μg) or OVA (250 μg) emulsified in CFA (Iatoron, Tokyo, Japan) in the hind footpads. On day 21, blood was obtained from the orbital venous plexus using a capillary tube and was allowed to clot at 4°C. Sera were stored at −20°C until analysis.

Antibody assay

Serum levels of IgG class anti-BGG antibodies were quantified using ELISA. ELISA plates were coated with 50 μL/well BGG and kept overnight at 4°C. Wells were blocked with 1% BSA in PBS at 37°C for 1 h, washed with PBS containing 0.05% Tween-20, and then incubated with 50 μL of serum samples serially diluted with PBS containing 1% BSA at 37°C for 1 h. The wells were then washed and incubated with 50 μL of goat anti-mouse IgG antibodies (1/5000) labeled with horseradish peroxidase (Zymed Laboratories, San Francisco, CA) in PBS containing 1% BSA at 37°C for 1 h. After washing, wells were developed with 2.8 mM *o*-phenylendiamine (Wako Chemicals, Osaka, Japan) in the presence of H_2O_2 (4.4 mM). The reaction was stopped with 2.5 N H_2SO_4 (50 μL), and absorbance at 490 nm was measured. A pool of sera obtained from B6 mice immunized with BGG was used as a standard serum pool containing one million units/mL of IgG class anti-BGG antibodies. Serum levels of anti-BGG antibodies are expressed in units, referring to a titration curve obtained by serial dilutions of the standard serum pool. Serum levels of IgG class anti-OVA antibodies were quantified using ELISA as for anti-BGG antibodies.

Serum levels of IgG anti-dsDNA antibodies were also measured using ELISA as described previously [14]. DNA was obtained from the calf thymus (Sigma Chemicals). DNA-binding activities are expressed in arbitrary units, referring to a standard curve obtained by the serial dilution of a standard serum pool from (NZB × NZW)F_1 mice over the age of 8 months, containing 1000 unit activities/mL.

Genotyping

Genomic DNA samples were extracted from tails. Polymorphism of microsatellite markers was analyzed by a modified version of the method described by Dietrich et al. [49]. Dye-labeled primer pairs were obtained from Applied Biosystems (Foster City, CA). PCR mixtures (7 μL) contained 120 nM each of forward and reverse primers, 2.5 mM of dNTP, 10 mM Tris-HCl (pH 8.3), 51 mM KCl, 1.5 mM $MgCl_2$, 4 μg/mL DNA, and 0.05 units/μL Taq polymerase (Invitrogen, Carlsbad, CA). The PCR amplifications were carried out using a GeneAmp 9700 PCR System (Applied Biosystems). The reaction consisted of initial denaturation at 94°C for 1 min, followed by 25 cycles of 94°C for 1 min, 56–58°C for 1.5 min, and 72°C for 10 min, and final extension at 72°C for 10 min. PCR products were analyzed using an ABI Prism 3700 DNA Analyzer (Applied Biosystems). A standard mixture of LIZ-labeled oligonucleotides (Applied Biosystems) was included in each run of the capillary electrophoresis. Sizes of the amplified microsatellite DNA were determined using GENESCAN and GENOTYPER software (Applied Biosystems).

For the genotyping of *Fcgr4* in two lines of FcγRIIB-deficient B6 mice, primers for PCR were designed to amplify the fragment containing *Fcgr4* SNPs of map position, Chr1:172948752, 172948763, 172948768, and 172948844, and PCR products were directly sequenced using the dideoxy chain termination method with *Taq* dye primer cycle sequencing kits (Applied Biosystems). Primers used were 5′-CAAACAACCAAACACACACAAA-3′ and 5′-ACCAAG GGGGATAGAACCAC-3′. Polymorphism of *Fcgr3* in B6-unique insertion and deletion sites of α-chain was determined by the length polymorphism of PCR product between 129 and B6, using 5′ primer,

5′-TCCATCTCTCTAGTCTGGTACC-3′ and 3′ primer, 5′-AAAA GTTGCTGCTGCCACC-3′. Polymorphisms of *Slam* families (*Cd229* and *Cd84*) were examined by single-strand conformational polymorphism. Primers for PCR were designed to amplify fragments encompassing the second exon of *Cd229* including amino acid position 130 and the second exon of *Cd84* including amino acid position 27. The 5′ and 3′ primers used were 5′-GCAGACTCAAAGTCAGC-GAAG-3′ and 5′-TGGTGAGGATAACATTCTTTTGG-3′ for *Cd229*, and 5′-AAAACAATTCAACAGTGTGATGG-3′ and 5′-AAGTCCAGGCAATG TTGTCA-3′ for *Cd84*. PCR products were denatured at 98°C for 10 min, loaded on an 15% polyacrylamide gel, and run in 0.5 × TBE employing a constant-temperature control system (AB-1600 and AE-6370, ATTO, Tokyo, Japan) at 17°C under a constant current of 20 mA/gel for 2 h. Single-stranded DNA fragments in the gel were visualized by silver staining (Daiichi Pure Chemicals, Tokyo, Japan).

Data analysis

Genomic interval mapping of QTL regulating the titers of antibodies in sera was performed using Map Manager software [50]. The criteria for the statistical significance of the linkage in genome-wide mapping [19] were empirically determined by permutation test using a program provided with the Map Manager package. The statistical variance analysis was done by Scheffe's method. Statistical analysis for the differences in antibody titers was carried out using Mann–Whitney *U*-test.

Acknowledgements: The authors thank Noriko Isoyama and Atsuko Kusano for the management of the mouse colonies and Noriko Iida for technical assistance. This work was supported in part by a Grant-in-Aid for Scientific Research (C) from the Ministry of Education, Culture, Sports, Science and Technology, Japan, a Grant-in-Aid (S0991013) from the Ministry of Education, Culture, Sports, Science and Technology, Japan, for the Foundation of Strategic Research Projects in Private Universities, and the Science Research Promotion Fund from the Promotion and Mutual Aid Corporation for Private Schools of Japan.

Conflict of interest: The authors declare no financial or commercial conflict of interest.

References

1 Goodnow, C. C., Sprent, J., Fazekas de St Groth, B. and Vinuesa, C. G., Cellular and genetic mechanisms of self tolerance and autoimmunity. *Nature* 2005. 435: 590–597.

2 Kronenberg, M. and Rudensky, A., Regulation of immunity by self-reactive T cells. *Nature* 2005. 435: 598–604.

3 Mitchison, N. A., Induction of immunological paralysis in two zones of dosage. *Proc. R Soc. Lond. B Biol. Sci.* 1964. 161: 275–292.

4 Weigle, W. O., Immunological unresponsiveness. *Adv. Immunol.* 1973. 16: 61–122.

5 Dresser, D. W., Specific inhibition of antibody production. II. Paralysis induced in adult mice by small quantities of protein antigen. *Immunology* 1962. 5: 378–388.

6 Chiller, J. M., Habicht, G. S. and Weigle, W. O., Cellular sites of immunologic unresponsiveness. *Proc. Natl. Acad. Sci. USA* 1970. 65: 551–556.

7 Chiller, J. M. and Weigle, W. O., Cellular events during induction of immunologic unresponsiveness in adult mice. *J. Immunol.* 1971. 106: 1633–1653.

8 Shirai, T., Hirose, S., Okada, T. and Nishimura, H., Immunology and immunopathology of the autoimmune disease of NZB and related mouse strains. In: Rihova, B. and Vetvicka, V. (Eds.), *Immunological Disorders in Mice*, CRC Press, Boca Raton, FL 1991. pp. 95–136.

9 Helyer, B. J. and Howie, J. B., Renal disease associated with positive lupus erythematosus tests in a cross-bred strain of mice. *Nature* 1963. 197: 197.

10 Jiang, Y., Hirose, S., Sanokawa-Akakura, R., Abe, M., Mi, X., Li, N., Miura, Y. et al., Genetically determined aberrant down-regulation of FcγRIIB1 in germinal center B cells associated with hyper-IgG and IgG autoantibodies in murine systemic lupus erythematosus. *Int. Immunol.* 1999. 11: 1685–1691.

11 Jiang, Y., Hirose, S., Abe, M., Sanokawa-Akakura, R., Ohtsuji, M., Mi, X., Li, N. et al., Polymorphisms in IgG Fc receptor IIB regulatory regions associated with autoimmune susceptibility. *Immunogenetics* 2000. 51: 429–435.

12 Ravetch, J. V. and Kinet, J-P., Fc receptors. *Annu. Rev. Immunol.* 1991. 9: 457–492.

13 Nimmerjahn, F. and Ravetch, J. V., Fcγ receptors: old friends and new family members. *Immunity* 2006. 24: 19–28.

14 Xiu, Y., Nakamura, K., Abe, M., Li, N., Wen, X. S., Jiang, Y., Zhang, D. et al., Transcriptional regulation of *Fcgr2b* gene by polymorphic promoter region and its contribution to humoral immune responses. *J Immunol.* 2002. 169: 4340–4346.

15 Wandstrat, A. E., Nguyen, C., Limaye, N., Chan, A. Y., Subramanian, S., Tian, X. H., Yim, Y. S. et al., Association of extensive polymorphisms in the SLAM/CD2 gene cluster with murine lupus. *Immunity* 2004. 21: 769–780.

16 Staples, P. J. and Talal, N., Relative inability to induce tolerance in adult NZB and NZB/NZW F1 mice. *J. Exp. Med.* 1969. 129: 123–139.

17 Laskin, C. A., Taurog, J. D., Smathers, P. A. and Steinberg, A. D., Studies of defective tolerance in murine lupus. *J. Immunol.* 1981. 127: 1743–1747.

18 Laskin, C. A., Smathers, P. A., Lieberman, R. and Steinberg, A. D., NZB cells actively interfere with the establishment of tolerance to BGG in radiation chimeras. *J. Immunol.* 1983. 131: 1121–1125.

19 Lander, E. and Kruglyak, L., Genetic dissection of complex traits: guidelines for interpreting and reporting linkage results. *Nat. Genet.* 1995. 11: 241–247.

20 Bolland, S. and Ravetch, J. V., Spontaneous autoimmune disease in FcγRIIB-deficient mice results from strain-specific epistasis. *Immunity* 2000. 13: 277–285.

21 Nimmerjahn, F. and Ravetch, J. V., Antibody-mediated modulation of immune responses. *Immunol. Rev.* 2010. 236: 265–275.

22 Takai, T., Ono, M., Hikida, M., Ohmori, H. and Ravetch, J. V., Augmented humoral and anaphylactic responses in FcγRII-deficient mice. *Nature* 1996. 379: 346–349.

23 Kono, D. H., Burlingame, R. W., Owens, D. G., Kuramochi, A., Balderas, R. S., Balomenos, D. and Theofilopoulos, A. N., Lupus susceptibility loci in New Zealand mice. *Proc. Natl. Acad. Sci. USA* 1994. 91: 10168–10172.

24 Vyse, T. J., Rozzo, S. J., Drake, C. G., Izui, S. and Kotzin, B. L., Control of multiple autoantibodies linked with a lupus nephritis susceptibility locus in New Zealand black mice. *J. Immunol.* 1997. 158: 5566–5574.

25 Haywood, M. E., Hogarth, M. B., Slingsby, J. H., Rose, S. J., Allen, P. J., Thompson, E. M., Maibaum, M. A. et al., Identification of intervals on chromosomes 1, 3, and 13 linked to the development of lupus in BXSB mice. *Arthtitis Rheum.* 2000. 43: 349–355.

26 Morel, L., Rudofsky, U. H., Longmate, J. A., Schiffenbauer, J. and Wakeland, E. K., Polygenic control of susceptibility to murine systemic lupus erythematosus. *Immunity* 1994. 1: 219–229.

27 Jørgensen, T. N., Alfaro, J., Enriquez, H. L., Jiang, C., Loo, W. M., Atencio, S., Gubbels Bupp, M. R. et al., Development of murine lupus involves the combined genetic contribution of the *SLAM* and *FcγR* intervals within the *Nba2* autoimmune susceptibility locus. *J. Immunol.* 2010. 184: 775–786.

28 Lin, Q., Xiu, Y., Jiang, Y., Tsurui, H., Nakamura, K., Kodera, S., Ohtsuji, M. et al., Genetic dissection of the effects of stimulatory and inhibitory IgG Fc receptors on murine lupus. *J. Immunol.* 2006, 177: 1646–1654.

29 Tsao, B. P., Lupus susceptibility genes on human chromosome 1. *Int. Rev. Immunol.* 2000. 19: 319–334.

30 Whitmer, K. J., Romball, C. G. and Weigle, W. O., Induction of tolerance to human γ-globulin in FcRγ- and FcγRII-deficient mice. *J. Immunol.* 1997. 159: 644–649.

31 Engel, P., Eck, M. J. and Terhorst, C., The SAP and SLAM families in immune responses and X-linked lymphoproliferative disease. *Nat. Rev. Immunol.* 2003. 3: 813–821.

32 Heszel, M., Detre, C., Rietdijk, S. T., Munos, P., Romero, X., Berger, S. B., Calpe, S. et al., A novel isoforms of the Ly108 gene ameliorates murine lupus. *J. Exp. Med.* 2011. 208: 811–822.

33 Komori, H., Furukawa, H., Mori, S., Ito, M. R., Terada, M., Zhang, M-C., Ishii, N. et al., A signal adaptor SLAM-associated protein regulates spontaneous autoimmunity and Fas-dependent lymphoproliferation in MRL-Fas^{lpr} lupus mice. *J. Immunol.* 2006. 175: 395–400.

34 Fukuyama, H., Nimmerjahn, F. and Ravetch, J. V., The inhibitory Fcγ receptor modulates autoimmunity by limiting the accumulation of immunoglobulin G^+ anti-DNA plasma cells. *Nat. Immunol.* 2005. 6: 99–106.

35 Pritchard, N. R., Cutler, A. J., Uribe, S., Chadban, S. J., Morley, B. J. and Smith, K. G., Autoimmune-prone mice share a promoter haplotype associated with reduced expression and function of the Fc receptor FcγRII. *Curr. Biol.* 2000. 10: 227–230.

36 Xiang, Z., Cutler, A. J., Brownlie, R. J., Fairfax, K., Lawlor, K. E., Severinson, E., Walker, E. U. et al., FcγRIIb controls bone marrow plasma cell persistence and apoptosis. *Nat. Immunol.* 2007. 8: 419–429.

37 Yuasa, T., Kubo, S., Yoshino, T., Ujike, A., Matsumura, K., Ono, M., Ravetch, V. J. et al., Deletion of Fcγ receptor IIB renders $H\text{-}2^b$ mice susceptible to collagen-induced arthritis. *J. Exp. Med.* 1999.189: 187–194.

38 Kleinau, S., Martinsson, P. and Heyman, B., Induction and suppression of collagen-induced arthritis is dependent on distinct Fcγ receptors. *J. Exp. Med.* 2000. 191: 1611–1616.

39 Johansson, A. C. M., Sundler, M., Kjellén, P., Johannesson, M., Cook, A., Lindqvist, A-K. B., Nakken, B. et al., Genetic control of collagen-induced arthritis in a cross with NOD and C57BL/10 mice is dependent on gene regions encoding complement factor 5 and FcγRIIb and is not associated with loci controlling diabetes. *Eur. J. Immunol.* 2001. 31: 1847–1858.

40 Chu, E. B., Hobbs, M. V., Ernst, D. N. and Weigle, W. O., In vivo tolerance induction and associated cytokine production by subsets of murine $CD4^+$ T cells. *J. Immunol.* 1995. 154: 4909–4914.

41 Murphy, E. D. and Roths, J. B., A Y chromosome associated factor in strain BXSB producing accelerated autoimmunity and lymphoproliferation. *Arthritis Rheum.* 1979. 22: 1188–1194.

42 Moll, T., Martinez-Soria, E., Santiago-Raber, M. L., Amano, H., Pihlgren-Bosch, M., Marinkovic, D. and Izui, S., Differential activation of anti-erythrocyte and anti-DNA autoreactive B lymphocytes by the Yaa mutation. *J. Immunol.* 2005. 174: 702–709.

43 Pisitkun, P., Deane, J. A., Difilippantonio, M. J., Tarasenko, T., Satterthwaite, A. B. and Bolland, S., Autoreactive B cell responses to RNA-related antigens due to *TLR7* gene duplication. *Science* 2006. 312: 1669–1672.

44 Subramanian, S., Tus, K., Li, Q., Wang, A., Tian, X. H., Zhou, J., Liang, C. et al., A Tlr7 translocation accelerates systemic autoimmunity in murine lupus. *Proc. Natl. Acad. Sci. USA* 2006. 103: 9970–9975.

45 Deane, J. A., Pisitkun, P., Barrett, R. S., Feigenbaum, L., Town, T., Ward, J. M., Flavell, R. A. et al., Control of Toll-like receptor 7 expression is essential to restrict autoimmunity and dendritic cell proliferation. *Immunity* 2007. 27: 801–810.

46 Heidari, Y., Bygrave, A E., Rigby, R. J., Rose, K. L., Walport, M. J., Cook, H. T., Vyse, T. J. et al., Identification of chromosome intervals from 129 and C57BL/6 mouse strains linked to the development of systemic lupus erythematosus. *Genes Immun.* 2006. 7: 592–599.

47 Davis, R. S., Dennis, G., Jr., Odom, M. R., Gibson, A. W., Kimberly, R. P., Burrows, P. D. and Cooper, M. D., Fc receptor homologs: newest members of a remarkably diverse Fc receptor gene family. *Immunol. Rev.* 2002. 190: 123–136.

48 Davis, R. S., Stephan, R. P., Chen, C. C., Dennis, G., Jr., and Cooper,M. D., Differential B cell expression of mouse Fc receptor homologs. *Int. Immunol.* 2004. 16: 1343–1353.

49 Dietrich, W., Katz, H., Lincoln, S. E., Shin, H. S., Friedman, J., Dracopoli, N. C. and Lander, E. S., A genetic map of the mouse suitable for typing intraspecific crosses. *Genetics* 1992. 131: 423–447.

50 Manly, K. F. and Olson, J. M., Overview of QTL mapping software and introduction to map manager QT. *Mamm. Genome* 1999. 10: 327–334.

Abbreviations: **BGG:** bovine γ globulin · **B6:** C57BL/6 · **DBGG:** deaggregated BGG · **DHGG:** deaggregated HGG · **FcγRIIB:** IgG Fc receptor IIB · **HGG:** human γ globulin · **LOD:** logarithm of odds · **NZB:** New Zealand Black · **NZW:** New Zealand White · **QTL:** quantitative trait loci · **SAP:** SLAM-associated protein · **Yaa:** Y chromosome-linked autoimmune acceleration

Full correspondence: Dr. Hiroyuki Nishimura, Toin Human Science and Technology Center, Department of Biomedical Engineering, Toin University of Yokohama, 1614 Kurogane-cho Aoba-ku, Yokohama 225-8502, Japan
Fax: +81-45-972-5972
e-mail: nisimura@cc.toin.ac.jp

Additional correspondence: Prof. Sachiko Hirose, Department of Pathology, Juntendo University School of Medicine, Tokyo, 113-8421, Japan
Fax: +81-3-3813-3164
e-mail: sacchi@juntendo.ac.jp

See accompanying Commentary:
http://dx.doi.org/10.1002/eji201141811

Received: 3/3/2011
Revised: 25/4/2011
Accepted: 20/5/2011
Accepted article online: 23/5/2011